Biochimica et Biophysica Acta 1848 (2015) 1729–1743

Contents lists available at ScienceDirect

Biochimica et Biophysica Acta

journal homepage: www.elsevier.com/locate/bbamem

Review

General and specific lipid–protein interactions in Na,K-ATPase☆

F. Cornelius [a,*], M. Habeck [b], R. Kanai [c], C. Toyoshima [c], S.J.D. Karlish [b]

[a] Department of Biomedicine, Aarhus University, Aarhus 8000, Denmark
[b] Department of Biological Chemistry, Weizmann Institute of Science, Rehovot 76100, Israel
[c] Institute of Molecular and Cellular Biosciences, University of Tokyo, Tokyo 113-0032, Japan

ARTICLE INFO

Article history:
Received 11 December 2014
Received in revised form 20 February 2015
Accepted 9 March 2015
Available online 16 March 2015

Keywords:
Na,K-ATPase phospholipid
Cholesterol
Reconstitution
Specific lipid–protein interactions
X-ray crystal structure
Recombinant Na,K-ATPase complexes

ABSTRACT

The molecular activity of Na,K-ATPase and other P2 ATPases like Ca^{2+}-ATPase is influenced by the lipid environment via both general (physical) and specific (chemical) interactions. Whereas the general effects of bilayer structure on membrane protein function are fairly well described and understood, the importance of the specific interactions has only been realized within the last decade due particularly to the growing field of membrane protein crystallization, which has shed new light on the molecular details of specific lipid–protein interactions. It is a remarkable observation that specific lipid–protein interactions seem to be evolutionarily conserved, and conformations of specifically bound lipids at the lipid–protein surface within the membrane are similar in crystal structures determined with different techniques and sources of the protein, despite the rather weak lipid–protein interaction energy. Studies of purified detergent-soluble recombinant αβ or αβFXYD Na,K-ATPase complexes reveal three separate functional effects of phospholipids and cholesterol with characteristic structural selectivity. The observations suggest that these three effects are exerted at separate binding sites for phophatidylserine/cholesterol (stabilizing), polyunsaturated phosphatidylethanolamine (stimulatory), and saturated PC or sphingomyelin/cholesterol (inhibitory), which may be located within three lipid-binding pockets identified in recent crystal structures of Na,K-ATPase. The findings point to a central role of direct and specific interactions of different phospholipids and cholesterol in determining both stability and molecular activity of Na,K-ATPase and possible implications for physiological regulation by membrane lipid composition. This article is part of a special issue titled "Lipid–Protein Interactions."

Contents

Abbreviations: CHL, cholesterol; $C_{12}E_8$, octaethylene glycol monodecyl ether; DDM, *n*-dodecyl-β-D-maltoside; DHA, decosahexaenoic acid; EP, phosphoenzyme; l_d and l_o, liquid-disordered and liquid-ordered phase; MD, molecular dynamic; n_c, number of carbon atoms in lipid acyl chains; PC, phosphatidylcholine; PE, phosphatidylethanolamine; PI, phosphatidylinositol; PL, phospholipid; PS, phosphatidylserine; PSD, phosphatidyl serine decarboxylase; PUFA, polyunsaturated fatty acids; SERCA, sarco(endo)plasmic reticulum Ca-ATPase; SM, sphingomyelin; TM, transmembrane.

☆ This article is part of a Special Issue entitled: Lipid–protein interactions.

* Corresponding author. Tel.: +45 8716 7746.
E-mail address: fc@biomed.au.dk (F. Cornelius).

http://dx.doi.org/10.1016/j.bbamem.2015.03.012
0005-2736/

1. Introduction

Integral proteins and lipids in biological membranes mutually affect each other. This has recently been underscored by quantitative evidence from non-equilibrium shape fluctuations in active membranes (Fig. 1), i.e., giant liposomes reconstituted with Na,K-ATPase, where dynamic flicker-noise analysis contain a relaxation time, which is comparable to the turnover time of Na^+-pumping [1]. Actually, the importance of lipid–protein interactions was appreciated long ago, and several recent reviews are available on the physical interactions of lipids and proteins [2–6], but our understanding of all the salient features of the lipid–protein interactions, especially the specific interactions, is only beginning to emerge. Thus, with the resolution of several lipids in crystal structures of membrane protein like the Na,K-ATPase [7,8], it is now realized that specific lipid–protein interactions have to be more closely considered, and functional studies of such interactions have already demonstrated remarkable conjunctions with recent structural observations [7–10]. It is therefore important to emphasize that membrane proteins like Na,K-ATPase are regulated by both *general lipid–protein interactions*, where the physical properties of the bilayer such as hydrophobic thickness, curvature stress, and elastic moduli affect the membrane protein conformational mobility and by *specific lipid–protein interactions*, where lipids interact chemically at lipid-binding sites located on the protein. The distinction, however, between the two types of interactions is often unclear. Typically, the general lipid–protein interactions are investigated in model systems, e.g., using reconstitution of Na,K-ATPase into liposomes of defined lipid composition [11,12], whereas specific lipid–protein interactions can be investigated in solubilized Na,K-ATPase lipid-detergent micelles where the physical constrains of a bilayer are more or less absent. Therefore, the two kinds of investigations may complement each other.

1.1. Native membranes are soft matter

The cell membrane is a lipid bilayer composed of an asymmetric disposition of a number of distinct lipid species, including cholesterol, containing adsorbed and integral membrane proteins. Lipid membranes are soft and allow proteins to change their lateral position and to adopt different shapes of their transmembrane (TM) domain during conformational changes. Moreover, the activation of Na,K-ATPase by ATP in the bilayer has been demonstrated to decrease the bending rigidity of the bilayer, i.e., it becomes even more soft by an amount equivalent to $7–8k_BT$, where k_B is Boltzmann's constant and T is the temperature in Kelvin, compared to membranes with inactive pump [1]. Indeed, physiological membranes are fluid, but in different ways. In the liquid-disordered (l_d) phase, the lipid fatty acid chains are conformationally disordered and the lipid molecules are spatially disordered, too, showing rapid lateral diffusion. Plasma membranes of animal cells contain, apart from phospholipids (PL), 30–50 mol% cholesterol (CHL), which in contrast to phospholipids is a fairly rigid molecule due to the steroid core. The presence of CHL restricts the conformational movements of adjacent fatty acid chains but retains the liquid nature of the bilayer allowing the lipids to be spatially disordered. Thus, CHL induces a so-called liquid-ordered (l_o) phase [13]. Due to this ordering of fatty acid chains, the bilayer thickness increases significantly by inclusion of

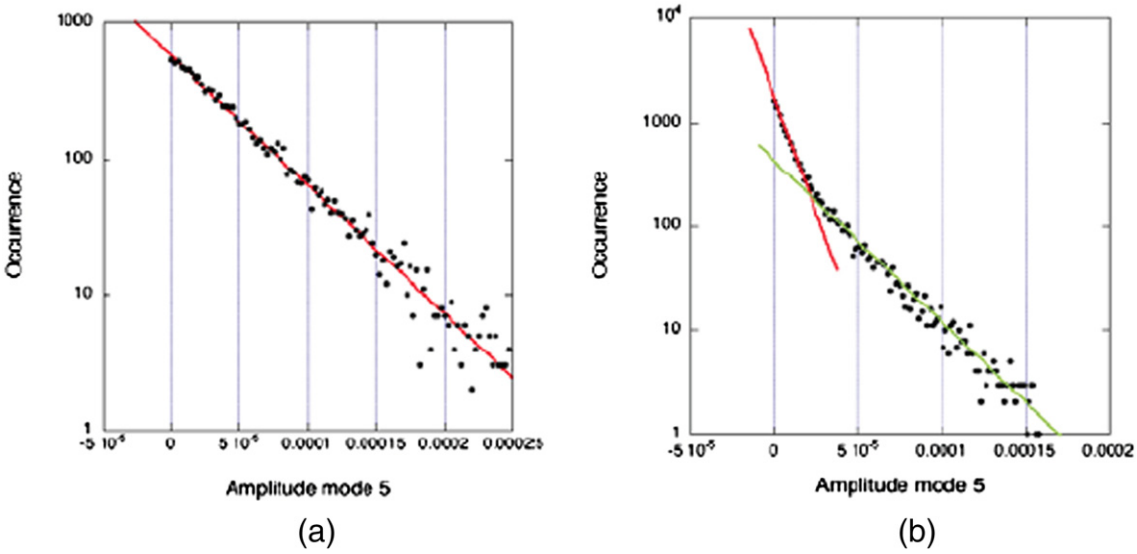

Fig. 1. Distribution of fluctuation amplitudes in GUVs reconstituted with Na,K-ATPase in the absence (a) and presence (b) of ATP. In the case where ATP is absent, the decay is monoexponential, as predicted, with a time constant dependent on the mode number. In the presence of ATP where the Na,K-ATPase is activated, the decay function is double exponential with a second time constant $\tau_2 \cong 0.5$ s that is independent of the mode number but equal to the time scale of the pumping cycle.

CHL. CHL also influences other important physical properties of the bilayer like elastic moduli and intrinsic curvature.

1.2. Bulk, annular, and specifically bound lipids

The first shell of lipids that coat the protein TM surface are termed *boundary or annular lipids* (orange spheres in Fig. 2). They are motionally restricted even though they exchange rapidly between positions along the protein TM surface and the bulk fluid phase (blue spheres in Fig. 2) at a rate of 10^6–10^7 s^{-1}, i.e., they exchange with the bulk lipids on a microsecond time scale [14,15]. For Na,K-ATPase, a little more than 30 lipids are annular [16,17], whereas the closely related Ca-ATPase has only about 20 annular lipids [18]. The composition of the annulus lipids of Na,K-ATPase is mainly PC and CHL with a few molecules of PS, whereas in Ca-ATPase it is mainly PC and PE. Thus, the presence of CHL, together with the additional two TM helices, may explain the larger number of annulus lipids in Na,K-ATPase compared to SERCA. The protein interaction with the annulus lipids varies. The shark Na,K-ATPase, e.g., has a higher specificity for anionic PL, especially PS, than for neutral [17]. Other lipids are more tightly associated with proteins in long-lived interactions that can be specific. Such lipids (red spheres in Fig. 2) are often found between α-helices of proteins, or in cavities on protein surfaces, and several PL's and CHLs have recently been resolved after crystallization of Na,K-ATPase [7,8,19]. They are referred to as *nonannular or specifically bound lipids*. Since the protein intramembrane surface is highly irregular, the specifically bound lipids are often significantly distorted to fit into grooves between the transmembrane α-helices, or between subunits (cf. Figs. 9–12).

2. General lipid–protein interactions

First, we will consider the lipid–protein interactions that depend on the lipid-induced changes in the physical properties of the bilayer that may influence the functional state of the incorporated proteins.

2.1. Hydrophobic matching and local deformations in bilayers during conformational changes

Membrane proteins span the membrane, and this transmembrane part of the protein, often in the form of a bundle of α-helices, is poor in polar residues (Fig. 3). The length of the hydrophobic core of the TM domain (l) should closely match the hydrophobic thickness of the membrane (d_0) in order not to expose non-polar residues to water. This is the so-called *hydrophobic matching principle* first proposed by Mouritsen and Bloom [20]. The hydrophobic core region of the plasma membrane corresponding to the acyl chains of the phospholipids is approximately 30 Å thick. On either side of the core a membrane interphase is situated about 12 Å thick corresponding to the phospholipid head groups. If a hydrophobic mismatch exists between l and the thickness of the unperturbed bilayer, the bilayer in the vicinity of the protein may deform by stretching/compressing and bending of lipids (Fig. 3). The elastic deformation energy, ΔG_{def}, will be dominated by the chain extension/compression associated with a bilayer deformation energy cost, which can be estimated by the semi-empirical equation: $\Delta G_{def} \cong 6.1 k_B T \frac{(l-d_0)^2}{d_0}$ per di-18:1 PC molecule [3]. If the constant 6.1 has unit nm^{-1} and the unit of lengths are in nm, ΔG_{def} has the unit kJ per lipid molecule. At 21 °C the equation thus becomes $\Delta G_{def} \cong 15 \frac{(l-d_0)^2}{d_0}$ in $kJ \cdot mol^{-1}$ of lipid. When a hydrophobic mismatch corresponding to a difference in acyl chain length of 5 carbons exists ΔG_{def} becomes about $1.5 k_B T$ per lipid compared, e.g., to the energy of a typical hydrogen bond of $5 k_B T$. The free energy related to bending distortion of the membrane surface normally is less significant, typically about 0.015–$0.035 k_B T$ per lipid [3], i.e., two orders of magnitude smaller than that

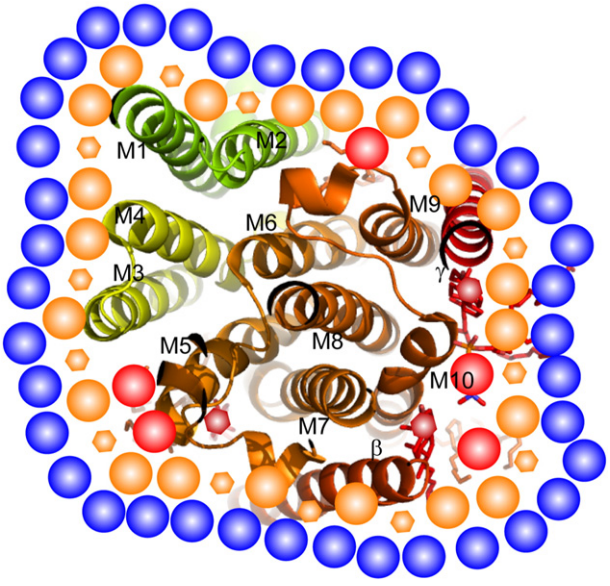

Fig. 2. Sketch showing location of annular and specific lipids. Cross section of the TM domain of Na,K-ATPase in the E1 ~ P·ADP·$3Na^+$ crystal (PDB ID:3WGV) as seen from the extracellular side of the membrane showing helices M1–M10 of the α-subunit, the β-subunit, and the γ. Colored spheres represent lipid head groups, polygons represent CHL. The first-shell lipids (here 34) are termed annular lipids (orange) and have very restricted mobility due to interaction with residues on the protein surface. 5 PC (red spheres) and 3 CHL (red polygons) are resolved in the crystal structure. They represent specifically bound lipids. Blue spheres indicate the bulk lipids with unrestricted mobility.

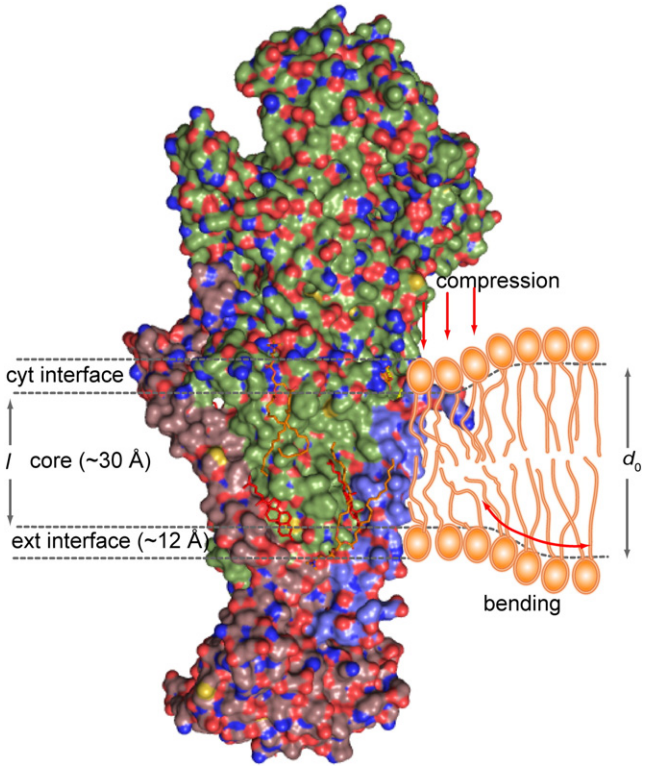

Fig. 3. Hydrophobic mismatch between the protein hydrophobic core with thickness l and the undistorted membrane hydrophobic thickness d_0 leading to compression and bending of the bilayer immediately adjacent to the protein. The Na,K-ATPase is shown as the water accessible surface (α-subunit green, β-subunit raspberry, and the γ blue) in atom color. Note that the surface of the core hydrophobic domain contains very few charged residues. The hydrophobic core is about 30 Å wide and sandwiched between the cytoplasmic (cyt) and extracellular (ext) membrane interface regions each about 12 Å wide containing many charged residues.

for chain stretching/compressing. Since proteins are much more rigid than membranes [2], it implies that the bilayer adjust to the protein and not vice versa, as depicted in Fig. 3. Nevertheless, the finite deformation energy may cause the integral proteins to fine-tune the conformations to better match the bilayer hydrophobic thickness as shown by MD simulations of Ca-ATPase in bilayers of different chain lengths, where it is apparent that hydrophobic mismatch induces both local deformations in the lipid bilayer and in the protein that adapts to the bilayer by small rearrangements of amino acid side chains and α-helix tilts [21], as also suggested by Andersen and Koeppe [2]. In SERCA1a, as the transmembrane helices move during turnover, the membrane thickness and residues interacting with PL head groups change, and even the orientation of the whole protein may change. This would result in large changes in cross-sectional area of the transmembrane region and lateral pressure of the lipids on the pump (see Section 2.3). It has also previously been clearly demonstrated that increasing CHL, which among other effects increases bilayer thickness, is able to shift the E2P/E1P conformational poise of Na,K-ATPase towards E1P [22] and the E2/E1 poise towards E1 [23].

The effects of lipid hydrophobic thickness on Na,K-ATPase activity have been investigated by reconstitution of Na,K-ATPase into liposomes produced from phospholipids of varying acyl chain length (n_C). Thus, the hydrophobic lipid thickness in nm, $\langle d_0 \rangle$ of PC with mono-unsaturated acyl chains in the liquid-crystalline phase, at 30 °C relates approximately to the number of carbons in the phospholipid acyl chain by the following relation: $\langle d_0 \rangle \cong 0.19(n_C - 3.9)$ [3].

In Fig. 4a, results are shown where Na,K-ATPase is reconstituted into liposomes produced from mono-unsaturated PL's of varying acyl chain lengths from 14 to 24 with or without 40 mol% CHL [12]. For each preparation, the amount of inside-out pumps was determined and the associated specific hydrolytic activity ($\mu mol \cdot mg^{-1} \cdot h^{-1}$) measured [11, 24]. As seen from the figure, maximum activity is observed at an n_C of 22 in the absence of CHL, corresponding to an average optimal hydrophobic bilayer thickness of $\langle d_0 \rangle = 3.82$ nm. When the same experiments were performed with liposomes containing 40 mol% CHL, the optimum is decreased to an n_C-value of 18, which also happens to be the average length of acyl chains in the native membrane [23]. This shift to shorter optimal chain lengths in the presence of cholesterol is compatible with the effect of CHL to increase acyl chain order and bilayer thickness. When the bilayer deformation energy ΔG_{def} is calculated assuming l equal to the bilayer hydrophobic thickness corresponding to $n_C = 18$ in the presence of CHL, it is observed that the ΔG_{def} distribution (stippled curve in Fig. 4a) is much broader than the activity profile. The increase in bilayer deformation energy, therefore, cannot alone account for the observed effect of varying acyl chain length on activity, indicating more specific effects of acyl chain lengths on Na,K-ATPase activity. Furthermore, it is also noted that cholesterol drastically increases the enzyme activity obtained at the optimal bilayer thickness without CHL. Indeed, CHL must have other, specific effects apart from the general physical effects on Na,K-ATPase activity through hydrophobic matching. Similar experiments have been performed using sarco(endo)-plasmic Ca-ATPase, SERCA1a [25]. Here the optimum acyl chain number in the absence of CHL was between 16 and 18 and the distribution much broader corresponding closely to the elastic deformation energy distribution. Endoplasmic reticulum contains much less CHL (about 10 mol%) than the plasma membrane. The closely related Na,K-ATPase and Ca-ATPase thus seem to have adapted to the different membrane environment they reside in. Another remarkable effect of bilayer thickness on SERCA is that when the mole fraction of di-14:1 PC relative to di-18:1 PC increased to more than 0.5 the Ca^{2+} binding stoichiometry of reconstituted SERCA1a apparently decreased from the ordinary 2 to only 1 [4,25]. It is possible that the decrease of membrane thickness induces a rearrangement of α-helix packing to disrupt one of the two Ca^{2+}-binding sites in SERCA.

2.2. Cholesterol

As previously mentioned, the animal plasma membrane contains 30–50 mol% CHL; in fact, all eukaryotes do, whereas it is absent in prokaryotes. Why is this sterol so important in our membranes? One reason, as previously mentioned, is that it imposes a high degree of conformational order on the phospholipid acyl chains thereby stabilizing the so-called liquid-ordered lipid phase [13]. This phase is still liquid, allowing rapid lateral diffusion in the membrane plane and at the same time confers mechanical stability to the bilayer by increasing the elastic moduli and bilayer thickness. These effects are unique to cholesterol whereas lanosterol, a closely related sterol with a less smooth steroid surface due to three additional methyl groups on the steroid core, is unable to induce the liquid-ordered lipid phase [26].

The cholesterol effects on the activation energy of Na,K-ATPase turnover can be evaluated by measuring the temperature dependence of the turnover number (k_{cat}) of the Na,K-ATPase reaction in liposomes with or without CHL. A plot of $\ln(k_{cat}/T)$ vs. $1/T$, the Eyring plot, may be linear provided that a single rate constant in reaction cycle is rate determining at the temperature range investigated. In this case, the values of $\Delta H^{‡}$ and $\Delta S^{‡}$, the enthalpy and entropy of activation, can be evaluated from the slope ($-\Delta H^{‡}/R$) and intercept ($\Delta S^{‡}/R + 23.76$). In Fig. 4b, the Eyring plots are shown for Na,K-ATPase reconstituted into liposomes with di-18:1 PC alone or together with 40 mol% CHL [12]. In both cases, a reasonable linear relationship is found, and $\Delta H^{‡}$ and $\Delta S^{‡}$ can be calculated from linear regression analysis to be $\Delta H^{‡} = 67.0 \pm 1.4$ kJ·mol^{-1} and $\Delta S^{‡} = -9.9 \pm 0.2$ J·K^{-1}·mol^{-1} in the absence of CHL and $\Delta H^{‡} =$

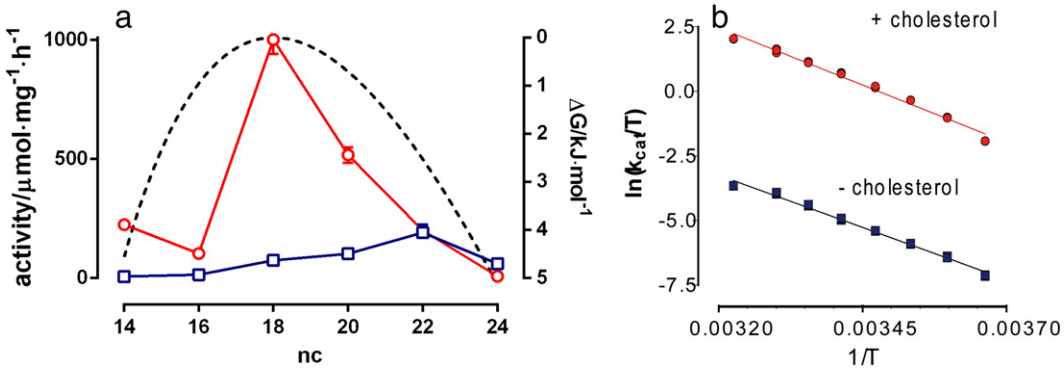

Fig. 4. (a) The specific hydrolytic activity of Na,K-ATPase reconstituted into liposomes of mono-unsaturated PL with acyl chain length between 14 and 24 plus 40 % CHL (red) or without CHL (blue). The stippled curve is the free energy of elastic deformation by acyl chain compression. (b) Eyring plots of activation energy of Na,K-ATPase reconstituted into di-18:1 PC with 40 mol% CHL (red) and without CHL (blue). Data from Cornelius 2001 [12].

73.7 ± 1.5 kJ·mol^{-1} and $\Delta S^{\ddagger} = 58.8 \pm 1.5$ J·K^{-1}·mol^{-1} in the presence of CHL, respectively. Thus, the enthalpy of activation is independent on the presence of CHL (slopes are the same), whereas the entropy of activation (from the intercepts) is negative in the absence of CHL but positive in its presence. This emphasizes that changes in physical property of bilayers induced by CHL are being dominated by changes in entropy. Increasing bilayer thickness, induced by using PC with longer acyl chains than for di-C18:1 PC, has a similar effect on $\Delta S^{\ddagger}$ as CHL when $n_C > 20$, indicating that this CHL effect manifests itself via the increased bilayer thickness. From the relation $\Delta G^{\ddagger} = \Delta H^{\ddagger} + T\Delta S^{\ddagger}$, the free energy of activation can be calculated for di-18:1 PC in the absence or presence of CHL to be 70.0 ± 1.5 and 56.2 ± 1.4 kJ·mol^{-1}, respectively, i.e., CHL reduces significantly the free energy of activation as the optimal bilayer thickness is achieved. $\Delta G^{\ddagger}$ depended on the bilayer thickness and is minimum at $n_C = 18$ in the presence of CHL, but at $n_C = 22$ in its absence. Thus, $\Delta G^{\ddagger}$ is minimum at a bilayer thickness that gives optimal turnover (Fig. 4a), and is also equal to $\Delta G^{\ddagger}$ of Na,K-ATPase in native membranes [23].

Obviously, the Na,K-ATPase, which is confined to the plasma membrane of animals, and the Ca-ATPase present in the endoplasmic reticulum must have adapted differently to the diverse membrane content of CHL. This is obvious already from the different optimal membrane thickness, where SERCA1a matches thinner membranes than Na,K-ATPase [4,12,25]. In Fig. 5a, the activity of Na,K-ATPase reconstituted into liposomes containing varying CHL content from 0 to 40 mol% is shown [27]. As seen, the hydrolytic activity is increased by CHL and is optimal at 20 mol% CHL, with a slight decrease in activity at 40 mol%. The increased activity is in accord with a CHL-induced increase in the rate determining E2 → E1 reaction step and a stabilization of the E1 conformation [23]. Actually, every reaction step we could measure in the Na,K-ATPase reaction cycle was found to be significantly affected by increasing concentration of CHL, including increased phosphoenzyme level, increased apparent ATP affinity, change in the cytoplasmic Na^+ activation with inhibition at high Na^+ concentrations, increasing rate of phosphorylation (Fig. 5b), and increased rate of spontaneous and K^+-activated dephosphorylation [23,27]. It seems improbable that one single general physical property of the bilayer like bilayer thickness could have such diverse impact on the enzyme reaction kinetics. Rather, it indicates that CHL has more specific impact on the Na,K-ATPase activity. This hypothesis now seems to be substantiated considerably by the finding of CHL molecules specifically bound to 3 different lipid-binding sites in the recent high resolution Na,K-ATPase crystal structures ([7,8] see paragraph 3).

Contrary to Na,K-ATPase, CHL seems to be excluded from the SERCA annulus lipids and SERCA1a is not activated by CHL [28–30], or is even inhibited by CHL especially in PE-containing lipid mixtures [31]. CHL does, however, interact with the TM surface and compete with PC for binding in reconstituted SERCA [18]. As previously mentioned, endoplasmic reticulum, where SERCA resides, contains significantly smaller amounts of CHL compared to the plasma membrane.

2.3. Polyunsaturated fatty acids as controller of curvature stress

Lipids containing polyunsaturated fatty acids (PUFA) like decosahexaenoic acid (DHA) with 22 carbons and 6 double bonds in the acyl chain have been shown to affect protein functions in several cases, most notably in the case of rhodopsin [32]. In shark Na,K-ATPase, it comprises 15 mol% of fatty acids [23]. With the very bulky acyl chains, this lipid has a propensity to form non-lamellar phases like the inverted hexagonal phase H_{II}. The resulting bilayer curvature stress may be mediated energetically to the protein structure via the so-called *lateral pressure profile*, which is a very fundamental physical property of lipid bilayers. The lateral pressure profile results from the very constrained state the lipids adopt when they are close together in a bilayer. It results from three forces inside the bilayer: a repulsive force between the lipid head groups that gives a positive pressure, hydrophobic forces acting at the hydrophobic-hydrophilic interface resulting in a negative pressure, and repulsive forces between the acyl chains of the fatty acids that give a positive pressure. At equilibrium, the net tension across the bilayer is zero, which means that the pressure between the acyl chains counteracting the two interface tensions becomes very large, typically several hundreds of atmospheres (Fig. 6).

The lateral pressure profile can couple to the protein structure and function via the stress it exerts on the protein TM domain if enzyme turnover involves variations in the protein cross-sectional area across the TM domain (Fig. 7). The work required to induce a conformational change between two states, *r* and *t*, of a protein relates to the lateral pressure profile, $\pi(z)$ by the equation [33]: $W = \int_z \pi(z)[A_t(z) - A_r(z)]dz$, demonstrating that the protein cross-sectional area in the two states, $A_t(z)$ and $A_r(z)$, must be different for the protein to sense the lateral pressure profile. As seen from Fig. 7, the cross-sectional area at the level of the cytoplasmic membrane interface is quite different for Na,K-ATPase in E1 ~ P and E2·P conformations.

When the turnover number of Na,K-ATPase reconstituted into liposomes containing 10 mol% of lipid with di-22:6 PC or 16:0–22:6 PC is measured, a significant decrease in turnover is observed. However, this inhibition is much less if 40 mol% CHL is also included (Fig. 8a). Thus, the Na,K-ATPase is inhibited in the presence of *n*-3 (ω-3) polyunsaturated PL, especially in the absence of CHL [34]. Also, the apparent Na^+-affinity is increased (Fig. 8b). The rigid cholesterol molecule with its smooth steroid surface does not mix well with polyunsaturated PL with their bulky lipid chains, and there is a tendency of CHL and polyunsaturated PL to laterally phase separate into DHA-poor/CHL-rich l_o-microdomains and DHA-rich/CHL-poor l_d-microdomains. The Na,K-ATPase may tend to be located to l_o/l_d-domain interfaces if interaction of the l_o- and l_d-domains with the Na,K-ATPase is more

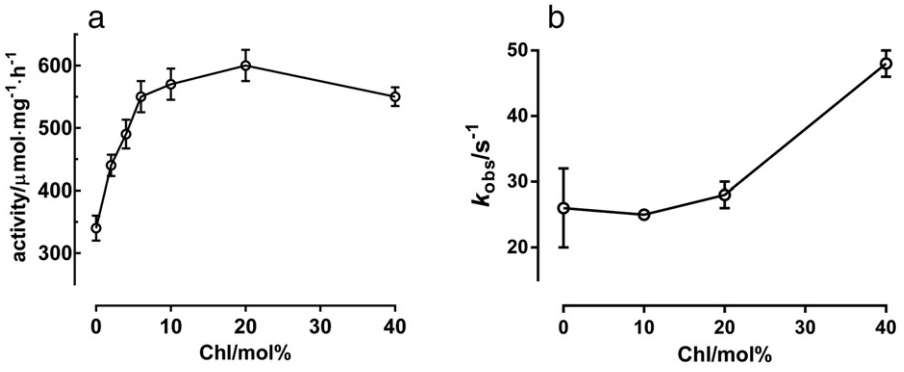

Fig. 5. The hydrolytic activity (panel a) and the rate of phosphorylation (panel b) of Na,K-ATPase reconstituted into di-18:1 PC liposomes with increasing CHL content. Data from Cornelius 1995 [27] and Cornelius et al. 2003 [23].

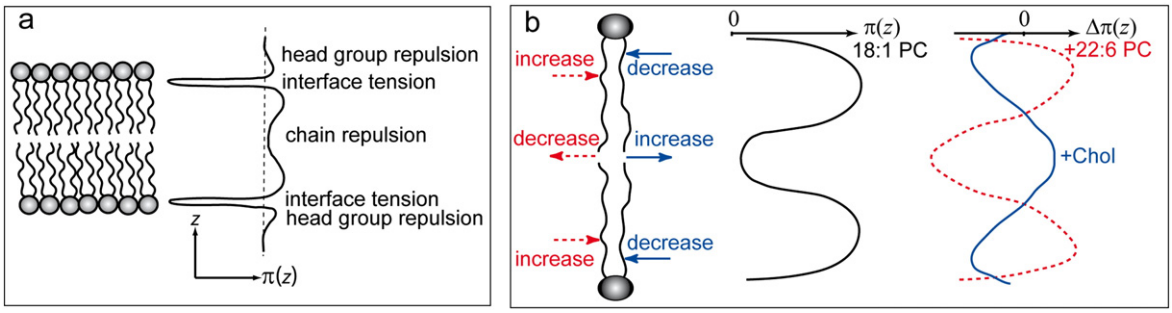

Fig. 6. (a) Lateral pressure profile in a symmetric bilayer. The forces that give rise to the pressure profile are repulsion of head groups, the interface tensions, and repulsive forces between the lipid chains. In panel b, the effects of CHL and 22:6 PC is indicated. CHL increases the lateral pressure in the middle of the bilayer and decreases it near the interfaces. 22:6 PC has the opposite effects. Redrawn from Cornelius 2008 [34].

favorable than with each other [35,36]. Thus, DHA inhibition of Na,K-ATPase could be the result of CHL exclusion near the pump surface. Finally, CHL and DHA are known to change the $\pi(z)$ profile through the bilayer (Fig. 6b). CHL increases the lateral pressure in the middle of the bilayer and decreases it near the interfaces, whereas DHA has the opposite effect, it increases pressure near the bilayer interfaces and decreases it in the middle [33,37]. Thus, changes in the structure of protein interfaces during conformational transitions associated with a change in cross-sectional area (Fig. 7) may be important.

3. Specific lipid–protein interactions—a structural view

In the first complete crystal structure of Na,K-ATPase from shark in the E2·Pi·2 K^+ conformation, a CHL molecule (CHL1) was resolved [7] in what is now designated lipid site C between the β and αM3, αM5, and αM7 (Fig. 7, Table 1). It is located at a position essential for stabilizing the kink in M7, which is important to make room for binding of the K^+-ions. Remodeling of the shark structure resolved, however, two additional PL's that can be modeled as PS and PC, respectively, in what was designated site A and B [9]. In the recent E1 ~ P·ADP·3Na^+ structure [8], CHL1 in lipid-binding site C is preserved, demonstrating that it is evolutionary conserved, and two additional CHL's are resolved (CHL2 near the β-subunit and CHL3 near the γ) plus 5 PL molecules positioned in 3 lipid-binding regions A, B, and C (Figs. 7, 9–12, Table 1). The PL electron density was continuous throughout the acyl chains indicating that these PL's are immobilized by tight association to the protein. The lipids are distorted to various degrees by binding in grooves at the protein surface. Since native lipids may be substituted by PCs added in the crystallization buffer, it is not known whether the PL's represent native PL's. Indeed, the structures strongly indicate the presence of specifically bound lipids to Na,K-ATPase as also previously inferred from X-ray structures of the closely related SERCA1a, where 5 different binding sites for PL head groups can be identified [38], some of which are homologous to the sites described here, V-type Na^+-ATPase [39], bacterial photosynthetic reaction center [40], bacteriorhodopsin [41], cytochrome *c* oxidase [42], and K^+-channel [43], among others (for a more comprehensive list, see reviews by Fyfe et al. [44]; Contreras et al. [5]).

In the Na,K-ATPase crystal structures, the CHL's are found to be H-bonded to protein residues in the membrane interface region, and the steroid core and acyl chain by hydrophobic interactions with non-polar residues. A general arrangement seems to be that the CHL molecules are all confined to deep grooves in the protein surface and at boundaries between subunits. Thus, CHL1 is positioned at the αβ interface on the cytoplasmic side (lipid site C), CHL2 at the αβ interface on the extracellular side (lipid site A3), and CHL3 at the αγ interface at the extracellular side (lipid site A2). The CHL's in the E1 ~ P state are covered by associated PL's. Also, the PL's are partly embedded in deep grooves in the protein surface. The PL head phosphodiester group and glycerol oxygens are coordinated by polar residues in the membrane interface regions (Table 1, Figs. 10–12) and the acyl chains by van der Waals interactions with surface-exposed hydrophobic residues in the TM

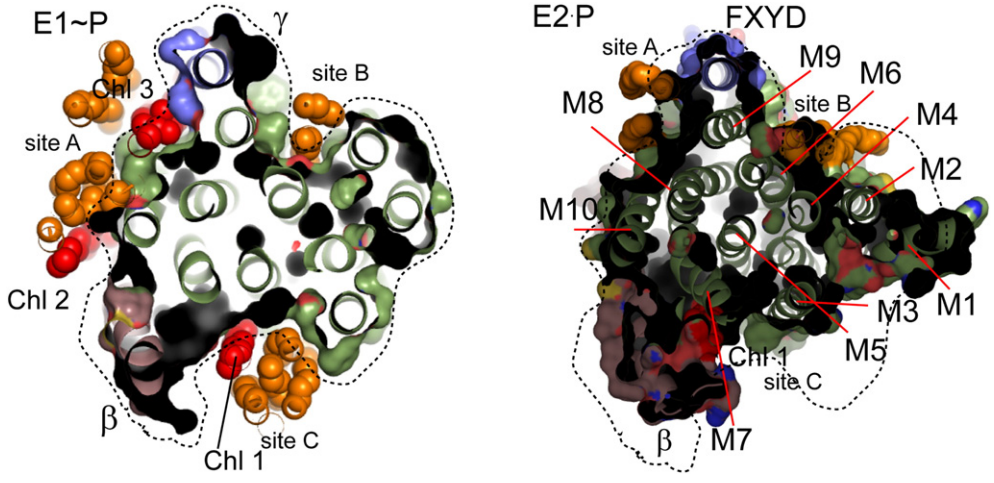

Fig. 7. Cross-sectional area of Na,K-ATPase in the pig kidney E1 ~ P·ADP·3Na^+ (PDB ID: 3WGV) and in shark E2·Pi·2 K^+ (PDB ID: 2ZXE) structures near the membrane interface at the cytoplasmic side. The protein perimeter in E1 ~ P·ADP·3Na^+ indicated by the stippled curve is also shown around the E2·Pi·2 K^+ structure for comparison. PL's (orange) are seen at lipid sites A, B, and C in E1 ~ P·ADP·3Na^+ from pig kidney, whereas the two PL's at site C are not resolved, or absent possibly due to the narrowing of the binding crevice in shark E2·Pi·2 K^+. However, a CHL (CHL1) molecule is conserved at similar positions in site C in both structures. In site B of E2·P, the groove around M1–M2 expands by a lateral movement of M1–M2, and the PL changes its conformation accordingly. Movements around M2 in the transition to E2·Pi·2 K^+ narrow lipid site B and the PL take up another position closer to the FXYD. The α-subunit is in green, β in raspberry, and FXYD in blue. PL's orange and CHL's red.

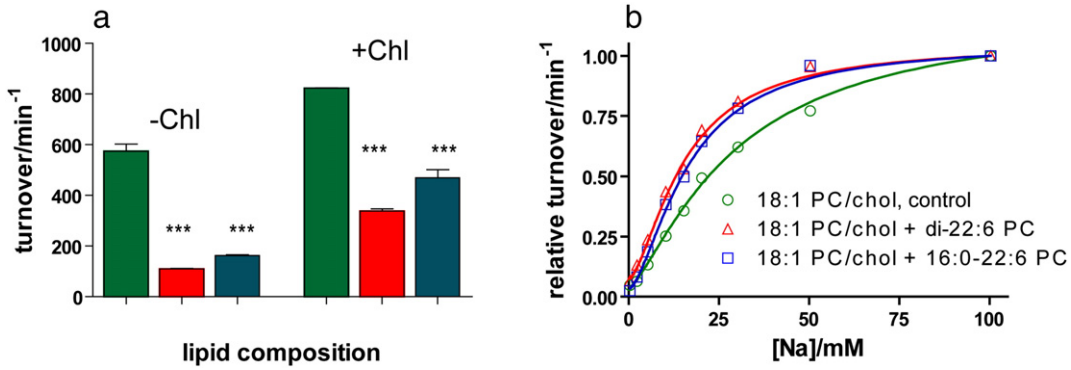

Fig. 8. Panel a shows that inclusion of 10 mol% di-22:6 PC (red) or 16:0–22:6 PC (blue) into di-18:1 PC (green) liposomes with reconstituted Na,K-ATPase results in a decreased maximum turnover both in the absence and presence of 40 mol% CHL. In panel b, it is shown that the apparent Na^+-affinity increases with addition of polyunsaturated PC to CHL-containing di-18:1 liposomes from a $K_{0.5}$ of 25 mM to about 15 mM. In liposomes without CHL, addition of polyunsaturated lipids did not affect apparent Na^+ affinity (not shown). Data from Cornelius 2008 [34].

core region. The key residues coordinating the specifically bound PL's and CHL's are shown in Table 1. Astonishingly, all the listed coordinating residues are conserved throughout the α1–α4 isoforms, except E840, which is a His, and K943, which is an Arg in α4.

3.1. Lipid site A—a composite site with four sub-sites

Lipid-binding site A is located between αM8-M10, FXYD, and β in the crystal contact area between two protomers. Lipid-binding sites A and B in the shark Na,K-ATPase as remodeled from 2ZXE are shown in Fig. 9a. The PL at site A is modeled as PS, probably carried over from the native lipids, whereas the one at site B is modeled as PC. The position of the PS head group in the shark enzyme very close to FXYD10 at the cytoplasmic membrane interface is interesting since acidic PL's have been shown to affect several kinetic properties of Na,K-ATPase including the ion-activation, the K^+-deocclusion, and the E1/E2 conformational equilibrium [45]. In Fig. 9b, lipid site A in the pig kidney crystal structure (PDB ID:3WGV) is shown. As seen, it is composed of 4 lipid-binding sub-sites A1, A2, A3, and A4 positioned between αM8, 9, 10, and FXYD. The PS found in the shark structure is located at site A1. In the pig structure, PCs are associated with CHL at sites A2 and A3 in protomer A and only at site A3 in protomer B. In this crystal, these PCs are shared with the ones at sites A1 or A4 of the other protomer due to the crystal packing. Lipids bound at crystal contact sites have previously been identified in various crystal structures of SERCA1a (reviewed in ref. [38]). Such association of PC with CHL bound to the protein may be important for function and/or stability of Na,K-ATPase. Lipid site A1 contains one PL modeled as PC in pig kidney enzyme, which is located at approximately the same position as PS in shark enzyme close to the FXYD10. The head group phosphodiester of shark PL in site A1 is within H- bonding distance from K950 and K452 (K943 and K945 in pig numbering). In pig kidney, Q940 and Q939 main chain carbonyls are within bonding distance of the PL phosphate oxygens, and M942 and V935 carbonyls are close to the glycerol hydroxyls (Fig. 10). In pig kidney, another PC on the opposite side of F938 is positioned in lipid-binding site A4. The PC head group in site A4 is coordinated by R1003 in αM10 and a glycerol hydroxyl by S936 side chain (Fig. 10, right panel). A PL has been modeled in SERCA1a at a homologous site [46], and the head group is there coordinated by R989 comparable to R1003 in Na,K-ATPase (PDB ID: 3AR3-7). In Fig. 9b, lipid sub-sites A2 and A3 are seen in pig kidney located at the extracellular membrane leaflet. In lipid site A2, a CHL3 is positioned in a deep pocket near the γ-subunit so that the CHL3 hydroxyl is coordinated by γV26. In lipid site A3, CHL2 is positioned also in a deep pocket close to the β-subunit. The hydroxyl of this CHL is coordinated by αE868 in M7 and by αT979 in M10. A CHL molecule equivalent to CHL3 at site A2 was also observed in the E2P-ouabain crystal structure (PDB ID: 4HYT) at a similar position [19]. The head group of the PL at site A2 is coordinated by βY68 and γY21, and the PL head group of PC in site A3 by βT60 main chain carbonyl.

In Fig. 10, the PL lipid-binding sites A1 in the shark (PS) and A1,A4 in pig structures (PC) are compared. The PS of shark enzyme and the PC of pig enzyme in lipid-binding site A1 are at almost identical positions although their conformations are slightly different. The A4 lipid-binding groove in the pig structure is much more confined than in the A1 sites of both shark and pig, and the bound PC is more distorted (Figs. 9 and 10). Also, the terminal part of the lipid acyl chains of this PL extends quite significantly from the protein surface (~10 Å).

3.2. Lipid-binding site B

Lipid-binding site B is located in the cleft between αM2, αM5, αM9, and FXYD. The lipid site of the two structures (shark PDB ID: 2ZXE and pig PDB ID: 3WGV) are compared in Fig. 11. The PL head group of the pig

Table 1
Characterization of the specific lipid-binding sites of Na,K-ATPase.

Lipid-binding site	State	Lipid	TM Location	Key coordinating residues	Leaflet	Functional role	References
A1	E2·P	PS	αM8-10, FXYD, β	K943, K945	Cyt	Stabilization	8–10, 54–56, 58, 59
	E1 ~ P	PC		Q939, Q940			
A2	E1 ~ P	PC	αM8-10, FXYD, β	K977, βY68, γY21	Ext	Stabilization	8, 10
		CHL3		γV26			
A3	E1 ~ P	PC	αM8-10, FXYD, β	βT60	Ext		8
		CHL2		E868, T979			
A4	E1 ~ P	PC	αM8-10, FXYD, β	R1003	Cyt		8
B	E2·P	PC	αM2,6,9, FXYD	K342	Cyt	Stimulation	8, 9, 10
	E1 ~ P	PC/PE		Y142,Q143, K146, Y817			
C	E2·P	CHL1	αM3,5,7, β	E1013*	Cyt		7, 8, 10
	E1 ~ P	2PC		T834		Inhibition?	
		CHL1		E840, βR27			

* Coordinating via a H_2O molecule. Numbering is according to pig kidney Na,K-ATPase sequence.

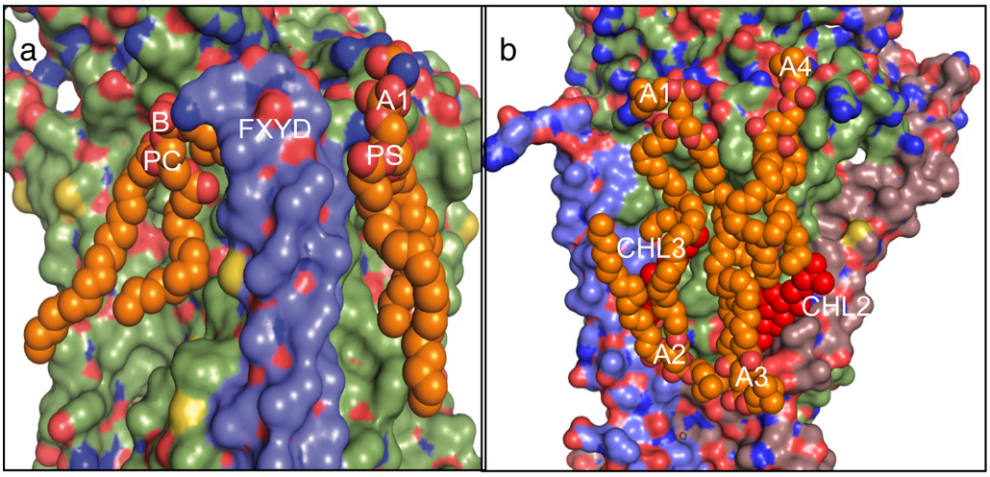

Fig. 9. Panel a shows lipid sites A1 and B in the crystal structure of shark Na,K-ATPase in the E2·Pi·2 K^+ crystal structure (PDB ID: 2ZXE). Remodeling of the 2ZXE structure resolved two phospholipids at the cytoplasmic side of the protein on either side of the FXYD10 designated lipid-binding sites A1 and B. The PL in site A1 is modeled as PS, and the one in site B as PC. In panel b, lipid site A of pig kidney is shown. In shark only one PL (PS) is resolved, whereas in pig there are 4 sub-sites: A1 and A4 on the cytoplasmic side containing each one PC molecule, and A2 and A3 on the extracellular side containing CHL3 and CHL2 each associated with a PC molecule. In the crystal structure site A of pig kidney, protomer A is in close contact with that of the neighboring protomer B in the next asymmetric unit. Due to the tight crystal packing, it is possible that the two protein units share lipids at the interface. α is colored green, β is raspberry, and FXYD is blue. PL's are orange and CHL's red.

enzyme is coordinated by several residues like Y142, Q143, and K146 on M2, as well as Y817 on the M6-M7 loop. In both structures, the lipid head group is very close to the FXYD protein. Several hydrophobic residues in M2 and M9 interact with the lipid acyl chains. The very narrow pocket forming lipid-binding site B in the pig structure (Fig. 11a,b) has expanded considerably in the shark E2·P structure due to the different positions especially of M1–M2 helices (Fig. 11c,d), as also previously described [9]. The PL has changed its conformation accordingly, and the PL head group has separated from the coordinating residues of M2 and is now coordinated by K349 (K342 in pig numbering). The E1 ~ P structure still hosts a PL in binding site B, now very distorted and compressed. In SERCA1a, a PC molecule is also observed here both in the E1Ca_2 and the E2 conformation [46] coordinated by Q108, a homologue of Q143 in Na,K-ATPase.

3.3. Lipid-binding site C

Lipid site C of pig kidney enzyme (PDB ID: 3WGV) is shown in Fig. 12. It is positioned in a very narrow pocket between αM3, αM5, αM7, and β. It hosts one CHL1, which is at a similar position as the CHL found in the shark crystal structure (PDB ID: 2ZXE), and in addition two stacked PL's modeled as PC. The head group of the innermost PL is coordinated by T834 main chain carbonyl and the glycerol hydroxyls are close to V838 and N839. E840 is contacting a glycerol hydroxyl of the outer PL as well as interacting with the hydroxyl of CHL1. The phosphate oxygen of the two PL head groups are within hydrogen bonding distance of each other. CHL1 in the two structures of shark and pig is positioned in a hydrophobic pocket mainly composed of hydrophobic residues from the β-subunit. The hydroxyl of CHL1 in the pig kidney

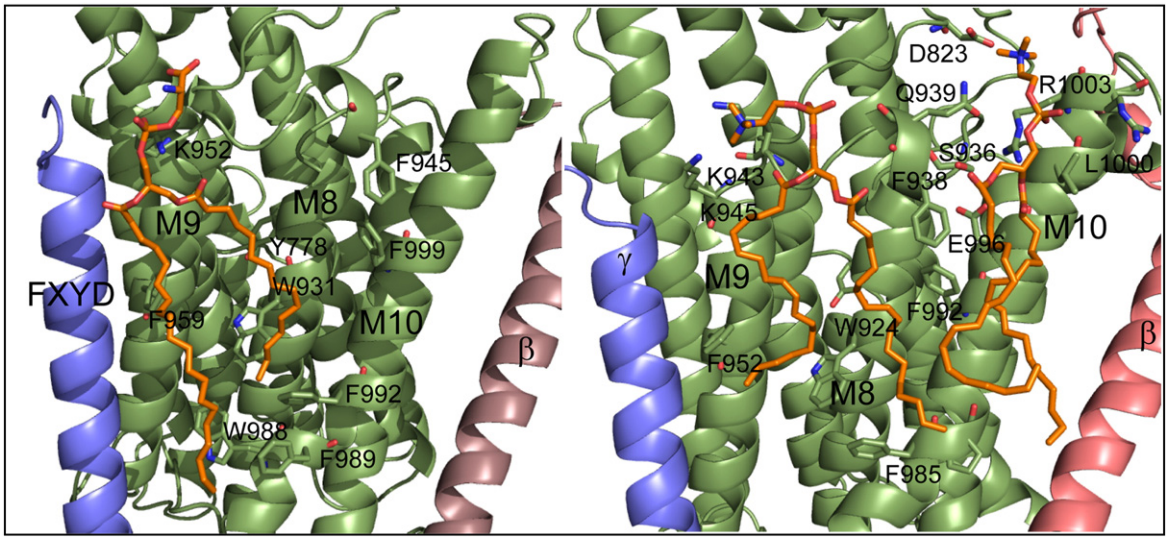

Fig. 10. Comparison of lipid site A1 in shark (left) and A1, A4 in pig kidney (right). The PC in pig kidney and PS in shark in site A1 are positioned almost at identical locations between αM8-M9, whereas PC in pig site A4 is on the other side of F938 (F945 in shark) between αM8 and M10. In shark the PS, head group is coordinated by K950 and K952 (K943 and K945 in pig), and the acyl chains lie in a hydrophobic pocket composed of W931, F992, F989, W988, F999, F959, and Y778 (shark numbering). In the pig structure, the PC head group in lipid site A4 is coordinated by R1003. The residues F938, F992, and F985 form the hydrophobic pocket (pig kidney numbering).

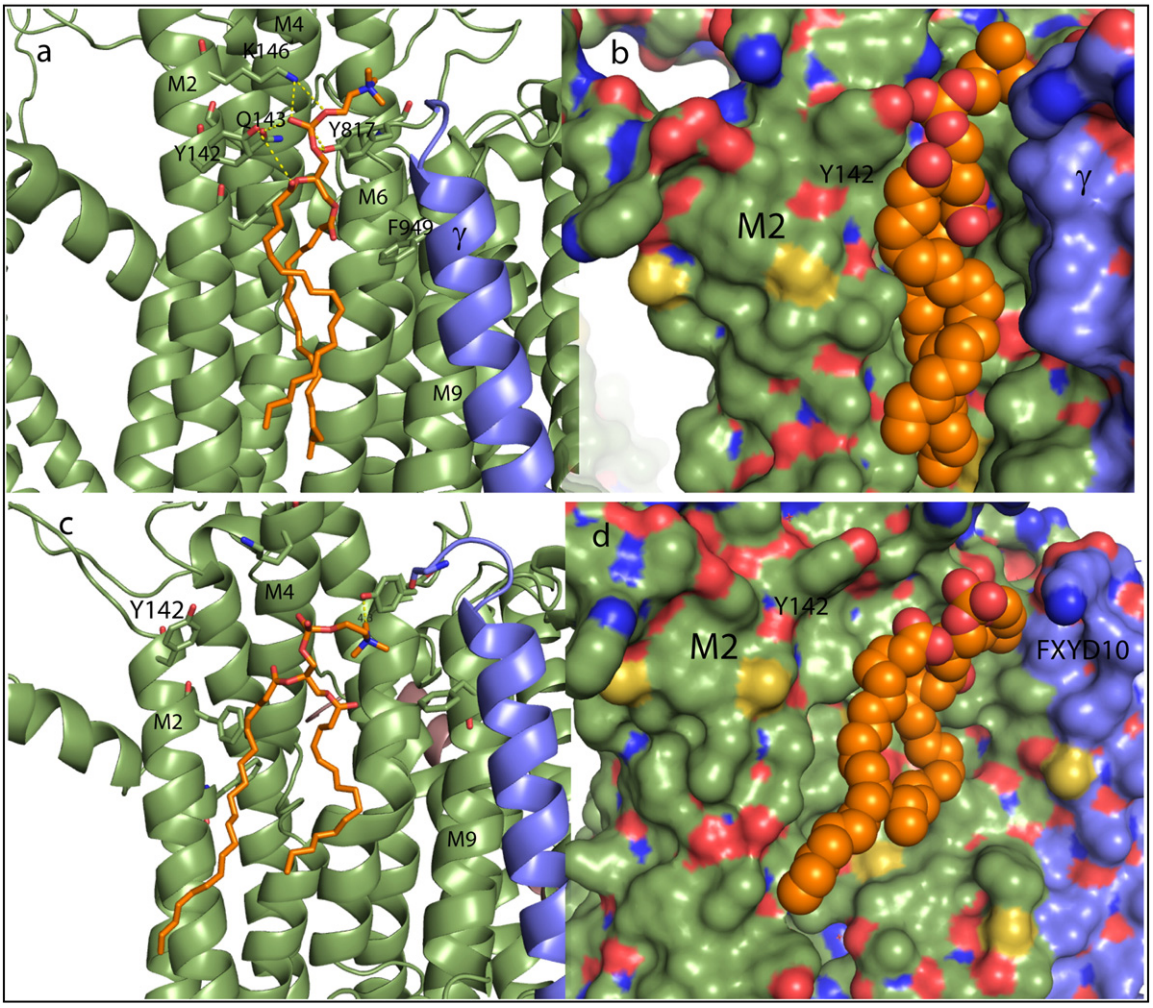

Fig. 11. Lipid site B. Panels a and b show pig kidney E1 ~ P·ADP·$3Na^+$ structure (PDB ID: 3WGV) with PL at site B squeezed into a narrow groove formed by α-helices M2, M4, M6, and M9 and the γ-subunit. The phosphate and glycerol oxygens interact with side chains of the polar and charged residue (sticks) at the cytoplasmic membrane interface region. The PL head group is coordinated by Y142 (M2), Q143 (M2), K146 (M2), and Y817 (M6). The hydrophobic pocket consists of residues like V132, I135, F139 of M2, V810, and I813 on M6, and I946 and F949 on M9. In panel b, the PC head is partly covered by the overhanging γ-subunit. Panels c and d show site B of the shark E2·P·$2K^+$ (PDB 2ZXE). The head group is no more coordinated by the M2 residues and is now coordinated by K349 (K342 in pig) in M4 and is only weakly interacting with Y824 (Y817 in pig). The acyl chains interact with hydrophobic residues like Y131, F146, and Y149 of M2, and F956 and F967 on M9. The binding cleft is expanded due to lateral displacement of M1–M2. The flexible PL (here modeled as a PC) adapts to the new crevice. Residues involved in interactions with the PL head groups are shown in stick.

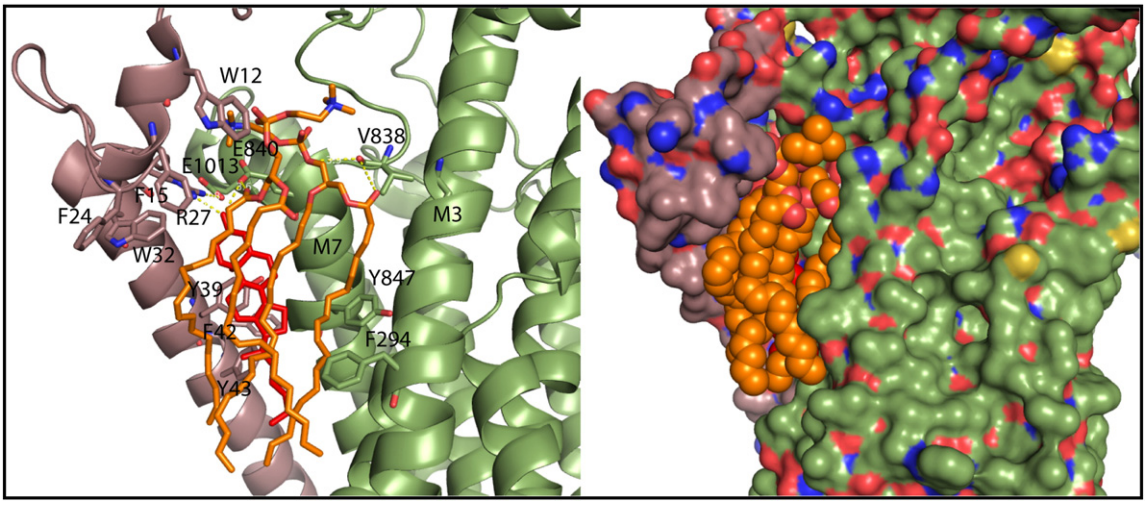

Fig. 12. Lipid site C of pig kidney Na,K-ATPase (PDB ID: 3WGV) containing CHL1 and two PLs in a very confined groove between the αM3, αM5, αM7, and β. In panel a, coordination of CHL and the PL's are shown, including βR27, αE840 (M7) side chains, and main chain carbonyl of αT834 and αV838 (M7). Several hydrophobic residues especially on the β-subunit participate in the hydrophobic pocket. In panel b, the surface is shown with the two PC molecules squeezed into the protein crevice between β (raspberry) and α (green) almost covering CHL1 (red).

structure is coordinated by E840 and βR27. In Fig. 12, left panel, coordinating residues are shown, and in the right panel, the surface is shown. As seen, γF15 and γW32 together with αF294 almost cover the site.

4. Functional effects and location of specifically bound lipids

In principle, lipids bound specifically to the Na,K-ATPase or other membrane proteins may affect protein stability, enzyme activity (activation or inhibition), ligand binding, protein–protein interactions, trafficking to and from the cell membrane and location in specific microdomains, or combinations of various effects (reviewed in [2–6]). While molecular structures of the Na,K-ATPase reveal phospholipids and cholesterol bound in pockets between transmembrane segments, detailed biochemical studies are required to define the functional roles and locations of particular lipids. Indeed, not all phospholipids and cholesterol seen in the structures may have specific functional roles.

Various findings from the older literature imply the existence of specific lipid-Na,K-ATPase interactions. As one very old example, based on a requirement for anionic phospholipids, especially phosphatidyl serine (PS), to maintain Na,K-ATPase activity of detergent-soluble brain microsomes, it was concluded that "the system for active transport of Na and K involves a complex unit of phosphatidylserine and the protein of the ATPase" [46]. Similarly, in order to maintain activity of detergent solubilized renal Na,K-ATPase separated on size-exclusion HPLC columns, it was necessary to add an anionic phospholipid, preferably PS, to the running buffer [47]. Furthermore, the PS affected oligomeric state [48], and there was some selectivity for synthetic 18:1–18:1PS [49], suggestive of a direct stabilizing interaction. In an extensive study using spin labeled lipids [15], anionic lipids such as cardiolipin and PS were inferred to bind more specifically to renal Na,K-ATPase than neutral lipids and fatty acids. Furthermore, binding of PS was preserved in extensively trypsinized Na,K-ATPase, in which the major cytoplasmic segments are removed but transmembrane segments and extracellular loops remain [50], suggesting that "the primary determinants of selectivity are preserved," most likely positively charged residues near the membrane surface [51]. It has been known for many years that cholesterol is required for optimal Na,K-ATPase activity as shown, for example, in [52] using renal membranes or in [27] using reconstituted proteoliposomes. The effects of cholesterol depletion or enrichment on Na,K-ATPase activity were interpreted either as due to bilayer effects [10] or specific cholesterol-Na,K-ATPase interactions [11]. The subsequent detailed study of effects of cholesterol and PCs of different chain lengths on Na,K-ATPase activity discussed above [12,23] implies that both bilayer effects and specific cholesterol-Na,K-ATPase interactions occur.

The examples just quoted are by no means exhaustive but, in any case, a more systematic study of specific lipid-Na,K-ATPase functional relations has become possible only with the development of purified detergent-soluble recombinant Na,K-ATPase, expressed at high levels in the methanotrophic yeast *Pichia pastoris* [53]. This system can provides mg quantities of ≈90% purified Na,K-ATPase, including various human or pig isoform combinations (α1His10β1, α2His10β1, α3His10β1, α2His10β3, α2His10β2) and mutants, prepared with different synthetic lipids and controlled lipid content [9,10,54–58]. After solubilization of the *P. pastoris* membranes in *n*-dodecyl-β-D-maltoside (DDM), purification is achieved by affinity chromatography on BD-Talon beads. The protein is eluted in a medium containing octaethylene glycol monodecyl ether ($C_{12}E_8$) or DDM and PS, without or with additional cholesterol and other phospholipids [54,55,57,58]. Regulatory FXYD proteins are expressed separately in *Escherichia coli*, purified and reconstituted spontaneously with the αβ complex and are eluted as αβFXYD complexes [56,59]. Several physical techniques show that the purified Na,K-ATPase consists mainly of monodisperse αβ or αβFXYD protomer complexes, detergent, and presumably bound phospholipids, with minor amounts of (α1β1FXYD1) di-protomers [10,54,55]. It is important to emphasize that the mixed protein–detergent–lipid micelles are fully soluble and can be centrifuged at high speed without precipitating or eluted on size-exclusion HPLC columns, and effects of added lipids are seen at rather low concentrations (<100 μM). This experimental set-up allows detection of specific lipid interactions based on their structural selectivity, dependence on cholesterol, effects of mutations, and other features, and avoids the inherent ambiguity in interpretation of lipid effects in experiments based on reconstituted lipid vesicle, namely, whether the effects are caused by specific lipid–protein interactions or by changes in physical properties of the bilayer.

4.1. Site A—stabilization by anionic lipids and cholesterol

In the absence of an anionic lipid in the wash and elution buffers, the purified recombinant Na,K-ATPase (α1β1) is inactive [55]. PS is superior to PI in supporting activity, while PC supports activity initially, but it is rapidly lost, and PE does not support activity at all. The selectivity for the anionic lipids resembles that for renal Na,K-ATPase [48], consistent with a stabilizing role of PS. The structural selectivity of the fatty acyl chains of PS provides strong evidence for a specific interaction [55]. As seen in Fig. 13a, human α1β1 made with synthetic PS having only saturated fatty acyl chains rapidly loses Na,K-ATPase activity, even at 0 °C. At least one double bond is required to maintain activity over time. Furthermore, 18:0–18:1PS is superior to 18:1–18:1PS at 0 °C and even more so at higher temperatures (>20 °C) [55]. Overall, the order of stabilizing effectivity is 18:0–18:1PS > 18:1–18:1PS ≈ 18:0–18:2PS > 18:2–18:2PS> > 14:0–14:0PS > 16:0–16:0PS ≈ 18:0–18:0PS. Fig. 13b shows that addition of cholesterol to the 18:0–18:1PS leads to strong additional stabilization although little activity is seen with cholesterol alone. The major yeast sterol ergosterol is a poor stabilizer. As seen in Table 2, the initial Na,K-ATPase activity for preparations made with 18:0–18:1PS, 18:1–18:1PS; 14:0–14:0PS 18:1–18:1PS/ cholesterol, and also 18:1–18:1PC without or with cholesterol are all equivalent and are quite independent of their ability to stabilize [55].

Evidently, anionic lipids such as 18:0–18:1PS, with or without cholesterol, stabilize activity but do not affect activity as such, at least in this system. Two observations suggested that cholesterol and the PS interact directly. First, in the presence of cholesterol the $K_{0.5}$ for 18:0–18:1PS is lowered from ≈ 50 μM to ≈ 25 μM. Second, cholesterol is less effective as a stabilizer in combination with 18:2–18:2PS compared to 18:0–18:1PS or 18:0–18:2PS [55]. Cholesterol is known to bind optimally to saturated acyl chains [60], making this observation understandable. An important observation is that the order of stability with different cations in the medium is $Na^+ > K^+ \approx Rb^+ > choline^+ > Cs^+ \approx Li^+$ [55]. This is indicative of selective stabilization by Na^+ ions (and not different stabilities of E1 and E2 conformations). Furthermore, the $K_{0.5}$ for 18:0–18:1PS prepared in media containing Na^+ is about 3-fold lower than in Na^+-free media (H. Haviv and S.J.D. Karlish, unpublished).

Ion mobility mass spectrometry is rapidly becoming an essential technique for detecting and characterizing specific lipid-binding sites on membrane proteins [61,62]. Indeed, we have recently applied this technique to the purified recombinant α1β1FXYD1 complex and obtained direct evidence for binding of one molecule of 18:0–18:1PS (M. Habeck, S.J.D. Karlish and M. Sharon unpublished work). This approach will become invaluable for testing hypotheses on lipid-binding sites, mutants etc.

Two sets of data indicate that PS/cholesterol bind in **pocket A** bounded by αM8-10/FXYD.

1. FXYD regulatory proteins are expressed in a tissue specific fashion and modulate kinetic properties of the Na,K-ATPase so as to adapt them to the needs of the cell, reviewed in [63,64]. Another function of FXYD proteins is to stabilize the Na,K-ATPase (both human α1β1 and α2β1) against thermal- and excess detergent-mediated inactivation [56,59]. Fig. 14a shows the protection of reconstituted α1β1FXYD complexes against thermal inactivation by purified FXYD proteins, with the order of effectiveness FXYD1 > FXYD2 > FXYD4 [59]. The mechanism involves amplification of the effect of PS,

Table 2
Initial Na,K-ATPase activities of α1β1 complexes prepared with different phospholipids and cholesterol.

Added PL	None	18:1–18:1PS	18:0–18:1PS	16:0–18:1PS	14:0–14:0PS	18:1–18:1PS/cholesterol	18:1–18:1PC	18:1–18:1PC/cholesterol
Na,K-ATPase, μmol/min/mg	1.7 ± 0.1	11.4 ± 1.0	11.9 ± 0.9	12.6 ± 1.2	11.5 ± 0.4	12.2 ± 1.0	11.9 ± 1.4	11.8 ± 0.3

probably due to direct binding of PS and the transmembrane segment of the FXYD protein, as inferred from several observations such as in Fig. 14b and c. Fig. 14b shows the FXYD proteins reduce the $K_{0.5}$ for 18:0–18:1PS in the order FXYD1 > FXYD2 ≈ FXYD4, to about 5–10 μM for FXYD1. Fig. 14c shows that the FXYD1 also strongly protects against inactivation by treatment with phosphatidylserine decarboxylase (PSD), an enzyme that converts PS to PE, which does not support Na,K-ATPase activity. In retrospect, an old finding that complete hydrolysis of PS by PSD does not inactivate renal Na,K-ATPase (α1β1FXYD2) might be explained by protection of the PS by FXYD2 [65]. Protection by FXYD proteins expressed in HeLa cells against thermal inactivation of Na,K-ATPase [58] and an observation that renal Na,K-ATPase in FXYD2 knock-out mice becomes thermolabile [66], showing that stabilization by FXYD proteins occurs also in mammalian cells. Taken all together, these findings provide a strong indication for a direct 18:0–18:1PS-FXYD1 interaction. As seen in Fig. 9, the transmembrane segment of the FXYD protein contacts phospholipids in both pocket A1 and B. Without further knowledge, either site could be a candidate for the selective interactions with PS.

2. Clear-cut evidence for the location of the 18:0–18:1PS and cholesterol stabilization site in pocket A has come from studies of the α2β1 isoform. α2β1 is a thermally unstable protein by comparison with α1β1 and α3β1 as shown both in yeast membranes expressing the three isoforms or the purified isoform proteins themselves [56,58], and also in rat heart membranes [58]. The origin of the relative instability was shown in [58] to be a weaker stabilizing interaction of α2β1 with 18:0–18:1PS compared to α1β1 and α3β1. A survey of residues unique to α2 compared to α1 and α3, focusing on transmembrane segments, revealed three residues in the pocket TM α2M8 (A920), M9 (L955), and M10 (V981) adjacent to TM FXYD. Fig. 15a depicts these residues, which have been mutated, singly or in combination, to the equivalent residues of α1 A920V, L955F, and V981P. Fig. 16a shows that while α2β1 is very unstable compared to α1β1, and single or double mutants have partial effects, the triple mutant referred to as α2VFPβ1, with all three substitutions to the α1 residues, shows thermal stability close to that of α1β1 itself [58]. Similar effects were seen for detergent-mediated inactivation. Furthermore, the α2VFP showed a higher "affinity" for 18:0–18:1PS compared to α2β1 and also for FXYD1 for stabilization against thermal inactivation, both properties being closer to those of α1β1. Significantly, α2VFPβ1 does not affect Na,K-ATPase activity or any enzyme kinetic properties compared to α2β1, consistent with these being purely stabilizing mutations. Another finding of interest is the identification of an unsaturated lactone, 6-penty-2-pyrone, isolated from a marine fungus, that acts as a 18:0–18:1PS antagonist and inactivates α2β1 at lower concentrations than α1β1 or α3β1, and again inactivation of α2FVPβ1 is more similar to α1β1 [58]. A recent and highly salient observation shown in Fig. 16b [10] is that the stabilization of α2VFPβ1 compared to α2β1 is much greater in the presence than absence of cholesterol ($t_{0.5}$ α2VFP/α2 2.4-fold versus 8.2-fold).

Conclusions from the findings in [10,58] and also [55] are that (a) the residues α2A920, L955, and V981 (or equivalent residues in α1 V917, F952, P978) collaborate to facilitate 18:0–18:1PS PS/ cholesterol mediated stabilization in pocket A; (b) 18:0–18:1PS and cholesterol interact directly and with the FXYD protein transmembrane segment pocket A to amplify stabilization compared to 18:0–18:1PS alone. A likely position of the relevant cholesterol (CHL3 in lipid sub-site A2, Fig. 9b) is indicated in Fig. 15b. CHL3 is in direct contact with α1P978 and indirect contact with α1V917, which impacts α1W981 that forms the direct contact with CHL3. F952, the third residue altered in α2VFP, does not contact the cholesterol but interacts with the FXYD protein (via V40, A37), which interacts directly with the cholesterol (via F33, G30, and V26). One likely candidate for the stabilizing PS is that in site A1 of the shark enzyme (Fig. 9A), which contacts the FXYD protein, faces the cytoplasmic surface as PS usually does, and may also come close enough to CHL3. The PL in site A4 of the renal enzyme (Figs. 9b and 10) is somewhat differently bound and is not in contact with the FXYD protein.

As proposed [10,58], the bound 18:0–18:1PS (in sub-site A1), CHL3 (in sub-site A2), and the FXYD protein, interacting with each other and the αM8-10 segments, seem to constitute a stability "hot spot" that maintains the topological stability of the αM8-M10 [20,21], which can be everted upon thermal destabilization [67,68,69]. A likely role of this "hot spot" is preservation of the unique Na^+ site III,

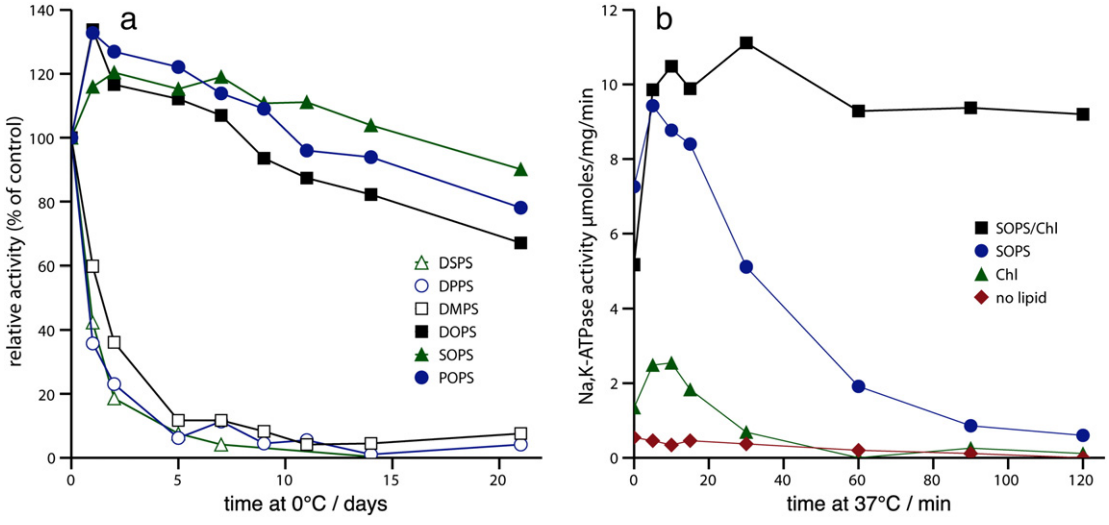

Fig. 13. Stability of human α1β1 Na,K-ATPase complexes prepared with (a) PS with different fatty acyl chains and (b) 18:0–18:1PS without or with cholesterol (ref [55]).

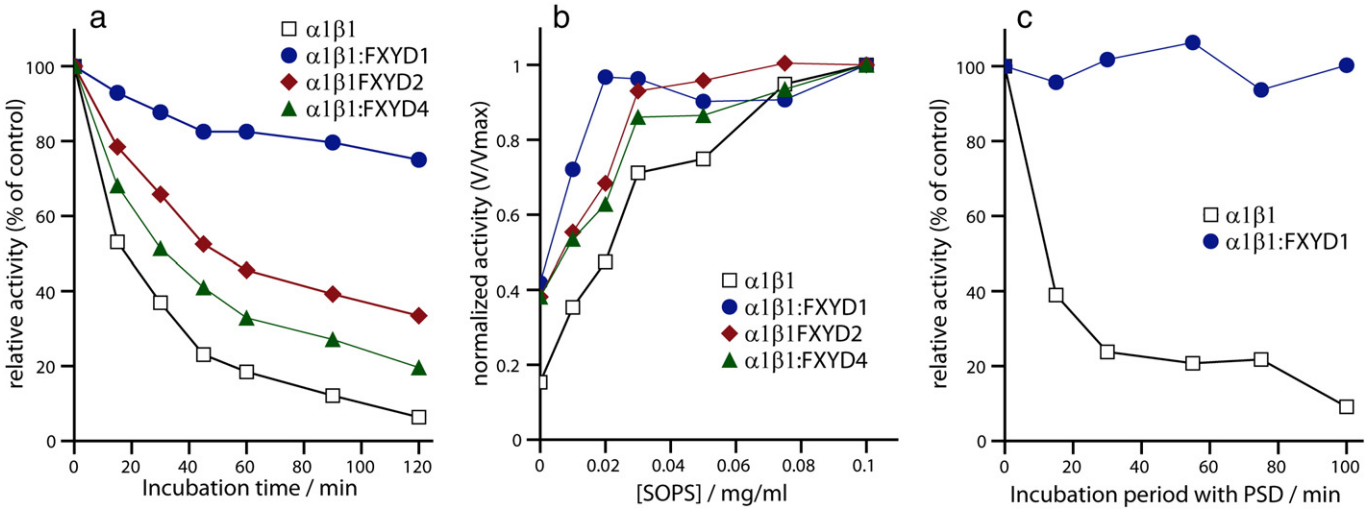

Fig. 14. (a) Thermal stability of human α1β1 Na,K-ATPase complexes reconstituted with FXYD proteins. (b) Dependence of Na,K-ATPase activity on 18:0-18:1Ps concentrations of human α1β1 complexes reconstituted with FXYD proteins. (c) Protection against phosphatidylserine decarboxylase of human α1β1 complexes reconstituted with FXYD1.

comprising residues from αM5, 6, and 8, which determines the selectivity and cooperativity of binding of the three Na^+ ions [8] (consistent also with the Na^+-selectivity for stabilization by 18:0–18:1PS [55]).

In shark rectal gland Na,K-ATPase, anionic lipids may play a different role to that in the renal and recombinant mammalian Na,K-ATPase. Anionic PL's affect several kinetic properties of Na,K-ATPase, including the ion-activation, the K^+-deocclusion, and the E1/E2 conformational equilibrium [45]. The PS head group is very close to FXYD10 at the cytoplasmic membrane interface, and interestingly, cross-linking experiments show that acidic PLs are important for the stabilization of FXYD-α interaction, probably due to interaction of the PS head group with a conserved cluster of basic residues on FXYD near the cytoplasmic membrane interface (K42, R44, and K46). This effect could be screened by addition of Ca^{2+} [45]. Possibly these effects, near FXYD10, are exerted from site B; see the next section.

4.2. Site B-stimulation by polyunsaturated neutral phospholipids (PE or PC)

Recently, we have described stimulation of Na,K-ATPase activity of the purified human α1β1 or α1β1FXYD1 complexes by neutral PUFA PC or PE [9,10]. In the presence of 18:0–18:1PS, soy PC (mainly 18:2–18:2PC) increases the molar Na,K-ATPase turnover rate from 5483 ± 144 to 7552 ± 105 min^{-1}. Analysis of α1β1FXYD1 complexes prepared with native or synthetic phospholipids shows that the stimulation is structurally selective for neutral phospholipids with polyunsaturated fatty acyl chains. Fig. 17 shows a detailed screen of the structural selectivity, showing that asymmetric 18:0–20:4 or 18:0–22:6 PE or PC are optimal, and can stimulate activity of human α1β1FXYD1 up to about 1.6-fold, about the same as natural brain PE (mainly 18:0–20:4 and 18:1–20:4 PE). By contrast, symmetric 18:2–18:2 PC and PE are like soy PC with a significant but lower effect, symmetric polyunsaturated 20:4–20:4 or 22:6–22:6 PE and PC are even less effective, and 18:0–18:1PC or PE have little or no effect. Human α2β1FXYD1 and α3β1FXYD1 isoforms are stimulated similarly to α1β1FXYD1 [10]. The structural selectivity for the neutral lipid class and asymmetric saturated plus PUFA fatty acyl chain structure is one strong indication for a specific interaction with the Na,K-ATPase. Stimulation by 20:4–20:4 PE or PC is quite independent of cholesterol and the FXYD protein, by contrast to stabilization by 18:0–18:1PS/cholesterol. The thermal stability in this preparation is somewhat lower than with 18:0–18:1PS/cholesterol with the order $K^+ > Na^+$, which contrasts with the order $Na^+ > K^+$ for the recombinant protein made only with 18:0–18:1PS/cholesterol, but it is similar to the renal Na,K-ATPase [70]. Other similarities of human α1β1FXYD1 made with 18:0–18:1PS/cholesterol/18:0–20:4PE to purified porcine renal Na,K-ATPase (α1β1FXYD2) include the maximal specific Na,K-ATPase of 30–35 μmol/min/mg protein, phosphoenzyme (EP) up to 5 nmol/mg

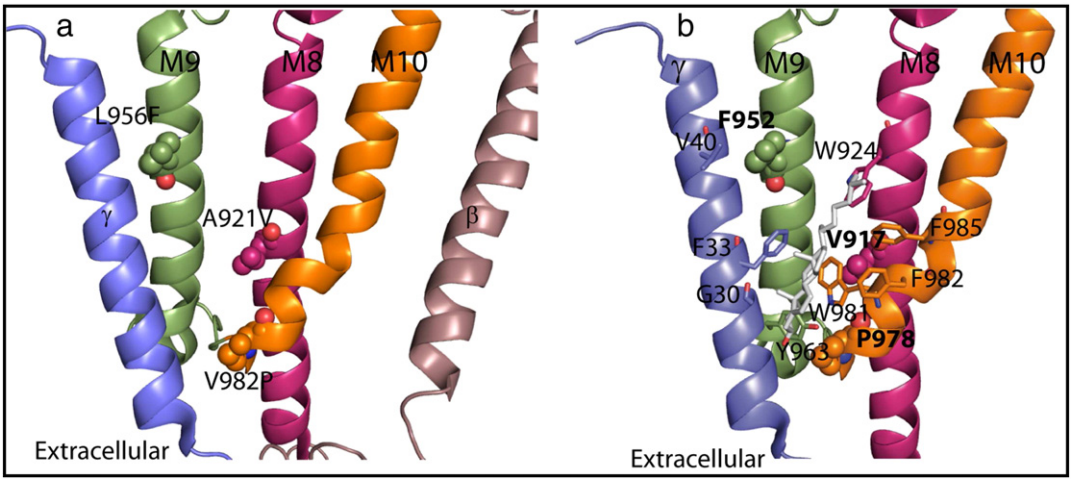

Fig. 15. (a) Design of mutants of α2 (L955F, A920V, and V981P singly or combined). (b) Cholesterol CHL3 (in sub-site A2) interacts with stabilizing residues.

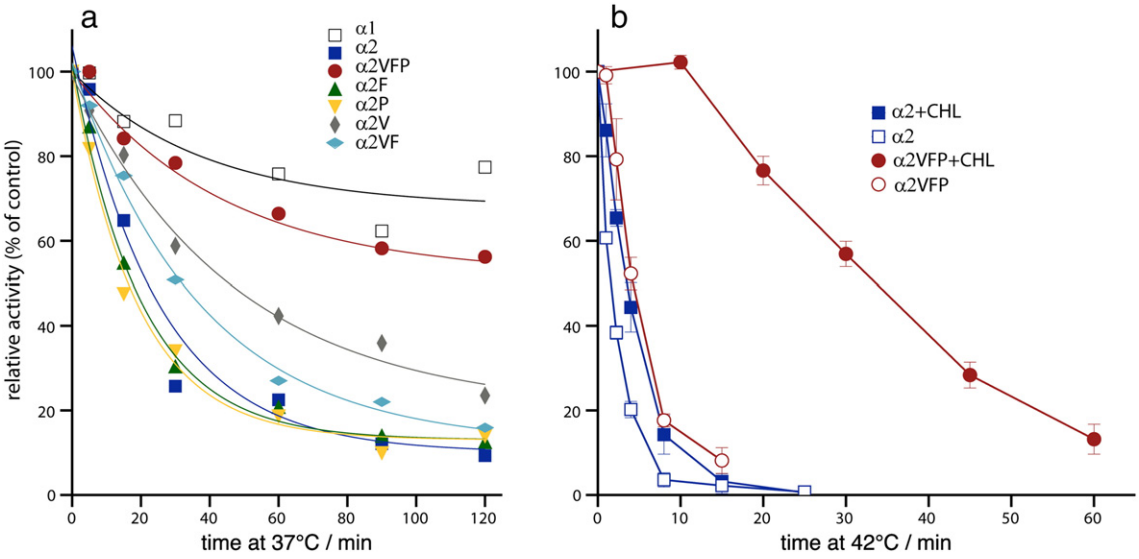

Fig. 16. (a) Thermal stability of α1β1 and α2β1 and single, double, or triple mutants of L955F, A920V, and V981P. (b) Thermal stabilization of triple mutant α2VFPβ1 is greatly amplified by cholesterol.

protein, and kinetic parameters such as $K_{0.5}$ Na^+, $K_{0.5}$ K^+, K_mATP, and $K_i$vanadate [71]. The structural selectivity for the stimulation by 18:0–20:4 or 18:0–22:6 PE or PC, as well as the distinct functional effects, and independence of cholesterol, makes it easy to distinguish these effects from the stabilization by 18:0–18:1PS/cholesterol. Evidently, the neutral PUFA phospholipids and 18:0–18:1PS occupy different sites.

Lipid site B is the optimal candidate to explain the stimulatory effects of 18:0–20:4 PE or 18:0–22:6 PE, as both the protein and lipid undergo conformational changes (and the site lacks cholesterol). As seen in Fig. 11, in the E1 ~ P conformation, the PL is located in a very narrow crevice between TM helices αM2, 4, 6 and 9, whereas in the E2·P structure, the lipid site expands considerable due to the different positions, especially of αM1–M2 helices and, accordingly, the PL expands to change its own conformation (Figs. 7 and 11). In this way, the PL may facilitate the E1P-E2P conformational transition (i.e., by lowering the activation energy). In the reverse conformational transition E2–E1, the conformation of the PL should readjust to fit back into to its binding site in the E1 conformation.

A recent photolabeling study of detergent-soluble renal Na,K-ATPase using [^{125}I]TID-PC/16 determined that the transmembrane domain of the Na,K-ATPase incorporates about 30% more label in the E2 conformation than in E1 conformation [72]. Although it was assumed that [^{125}I]TID-PC/16 is non-selective and, therefore, the degree of incorporation reflects lipids bound in the annular layer, the assumption of non-selective labeling would predict a approximately 30% increase in exposure of transmembrane segments to the surroundings in the E2 conformation. Since the crystal structures show clearly that this is not the case, it is likely that the [^{125}I]TID-PC/16 labeling is more selective than assumed (i.e., reacting with a relatively small number of residues). Indeed, by identifying labeled residues, it should be possible to identify the moving transmembrane segments of the pump and compare them to those identified in crystal structures in E1 and E2 conformations.

4.3. Site C inhibition by saturated PC or sphingomyelin

Fig. 18 shows that for preparations of the human α1β1FXYD1 complex made with all saturated phospholipids, and sphingomyelin (SM) Na,K-ATPase activity is inhibited up to 80% compared to the preparation made with PS/cholesterol alone [10]. The selectivities for the head group and fatty acyl chain length are in the order PC > PE > PS and 22:0 < 20:0 ≈ 18:0 > 16:0 > 14:0, respectively. Also, brain and egg sphingomyelin with choline head groups and major fatty acyl chain 18:0 and 16:0, respectively, inhibit by about 70%. An important feature is that cholesterol is required for the optimal inhibition (inhibition

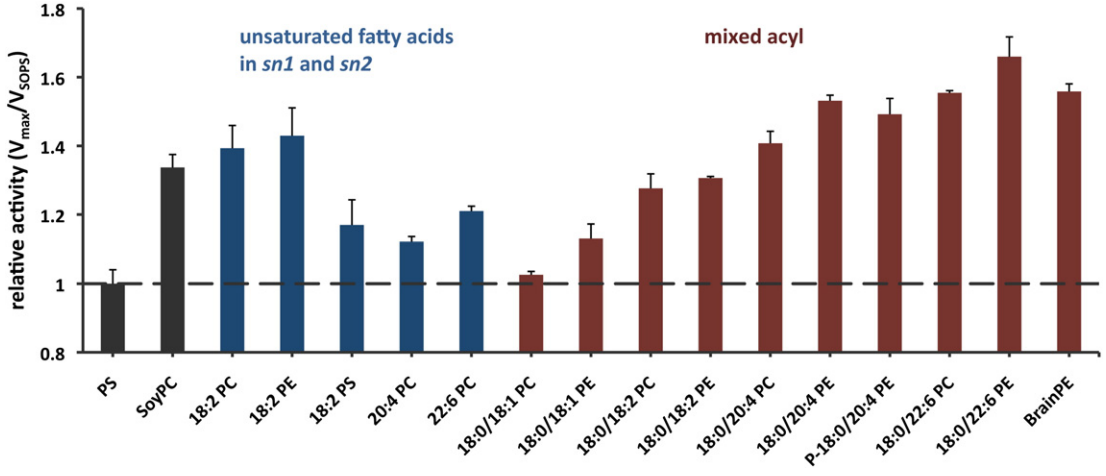

Fig. 17. Structural selectivity of neutral phospholipids (PE or PC) for stimulation of Na,K-ATPase activity of human α1β1FXYD1 complexes.

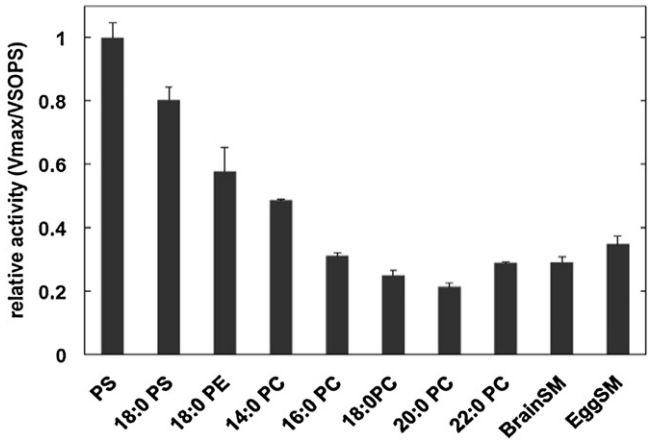

Fig. 18. Structural selectivity of phospholipids with saturated fatty acyl chains or sphingomyelin for inhibition of Na,K-ATPase activity of human α1β1FXYD1 complexes.

being only about 40% in the absence of cholesterol). Other important features are a lack of competition with PUFA PE and, in addition, when preparations are made with different proportions of brain PE and brain SM the activity can vary over a 10-fold range. These selectivity features distinguish this effect from the stimulation by PUFA neutral PL's and stabilization by 18:0–18:1PS/cholesterol and are consistent with a specific interaction of saturated PC or SM/cholesterol at a separate inhibitory binding site.

Since the inhibitory effect of saturated PC/SM is greatly amplified by cholesterol, and although there is no direct evidence, a possible site is close to the cholesterol molecule (CHL1) in the binding pocket C bounded by β, αM7 and αM3 (Fig. 12). The pocket accommodates two phospholipid molecules, one in close contact to the cholesterol, and it is conceivable that in some circumstances an inhibitory lipid could fit in next to the cholesterol. CHL2 and CHL3 in pocket A are less likely to be involved in inhibition since the αM 8,9,10 helices of the α-subunit undergo few if any movements during the reaction cycle. Also, CHL3 appears to be involved in stabilization.

A detailed analysis of kinetic mechanisms of both stimulatory effects of 18:0–20:4PE and inhibitory effects of brain SM shows that both classes of lipid stabilize E2 conformations of the protein but they do so by different mechanisms [10]. 18:0–20:4PE stimulates the rate of E1P-E2P, as suggested by the E1 and E2 structures in Fig. 11, whereas brain SM inhibits the rate of E2(2 K^+)ATP-E13Na^+ATP. In this way, 18:0–20:4PE stimulates or brain SM inhibit the Na,K-ATPase turnover rate, respectively, from the presumed different sites.

4.4. Physiological roles of specifically bound phospholipids and cholesterol?

If we assume that the specific lipid–protein interactions observed with the purified proteins and synthetic lipids reflect interactions that can occur in vivo, they could represent evolutionary adaptations of the pump to its immediate lipid environment that provide optimal stability or activity. Specific example of all three effects of the lipids, stabilization, stimulation, or inhibition are discussed at greater length in [10]. In relation to native cell membranes, which contain a much higher percentage of PUFA PE (or PE plasmalogen) compared to PC, the more likely "native" stimulatory lipid is PUFA PE, and, similarly, because native membrane contains only low amounts of all saturated PC but relatively large amounts of 18:0SM or 16:0SM, SM is the more likely "native" inhibitory lipid [10,73]. Of course, stimulatory and inhibitory effects of lipids are unlikely to co-exist in the same pump molecule. Thus, an inhibitory effect of SM/cholesterol, independent of the PE-interaction, could imply the possibility of a pool of inactive or non-pumping Na,K-ATPase under some physiological conditions- for example in SM/cholesterol-rich microdomains [74]. Accordingly, the activity of the pump could be regulated depending on the relative percentage of stimulatory and inhibitory lipids in the membrane and its compartmentalization in different domains.

5. Conclusion

It is remarkable that three different PL's and cholesterol binding pockets (A, B, and C) are observed in the crystal structures of Na,K-ATPase, and three separate functional effects have been detected: phophatidylserine/cholesterol (stabilizing), polyunsaturated phosphatidylethanolamine (stimulatory), and sphingomyelin/cholesterol (inhibitory). Of course, the hypothesis that these effects are mediated by lipids bound in sites A, B, and C must now be tested more systematically by mutating the putative PL/cholesterol binding residues. It is also possible that different bound lipids will be seen as more crystal structures become available. Nevertheless, the concept that direct and specific interactions of particular lipids determine both stability and activity of the Na,K-ATPase, in parallel with the indirect effects of bilayer structure, represents a novel paradigm for lipid–protein interactions of the pump. It may also serve as a precedent for other membrane proteins.

Conflict of interest

No conflicts of interests.

Acknowledgments

We thank Bianca Franchi and Hanne Kidmose for technical assistance. This work was supported by The Danish Medical Research Council and by the Novo Nordisk Foundation (to FC). We thank the Minerva Foundation for providing MH's fellowship.

References

[1] H. Bouvais, F. Cornelius, J.H. Ipsen, O.G. Mouritsen, Intrinsic reaction-cycle time scale of Na+, K+-ATPase manifests itself in the lipid–protein interactions of nonequilibrium membranes, Proc. Natl. Acad. Sci. U. S. A. 6 (2012) 18442–18446.
[2] O.S. Andersen, R.E. Koeppe, Bilayer thickness and membrane function: an energetic perspective, Annu. Rev. Biophys. Biomol. Struct. 36 (2007) 107–130.
[3] D. Marsh, Protein modulation of lipids, and vice versa, in membranes, Biochim. Biophys. Acta 1778 (2008) 1545–1575.
[4] A.G. Lee, Lipid–protein interactions, Biochem. Soc. Trans. 39 (2011) 761–766.
[5] F.-X. Contreras, A.M. Ernst, F. Wieland, B. Brügger, Specificity of intramembrane protein–lipid interactions, Cold Spring Harb. Perspect. Biol. 3 (2011) a004705.
[6] F. Cornelius, Active Biomimetic Membranes, in: C. Helix-Nielsen (Ed.), Biomimetic Membranes for Sensor and Separation Applications, Springer, 2012, pp. 113–135.
[7] T. Shinoda, H. Ogawa, F. Cornelius, C. Toyoshima, Crystal structure of the sodium-potassium pump at 2.4 Å resolution, Nature 459 (2009) 446–450.
[8] R. Kanai, H. Ogawa, B. Vilsen, F. Cornelius, C. Toyoshima, Crystal structure of a Na+-bound Na+, K+-ATPase preceding the E1P state, Nature 502 (2013) 201–206.
[9] H. Haviv, M. Habeck, R. Kanai, T. Toyoshima, S.J.D. Karlish, Neutral phospholipids stimulate Na,K-ATPase activity. A specific lipid–protein interaction, J. Biol. Chem. 288 (2013) 10073–10081.
[10] M. Habeck, H. Haviv, A. Katz, E. Kapri-Pardes, S. Ayciriex, A. Shevchenko, H. Ogawa, C. Toyoshima, S.J. Karlish, Stimulation, inhibition or stabilization of Na, K-ATPase caused by specific lipid interactions at distinct sites, J. Biol. Chem. 290 (2015) 4829–4842.
[11] F. Cornelius, J.C. Skou, Reconstitution of ($Na^+ + K^+$)-ATPase into phospholipid vesicles with full recovery of its specific activity, Biochim. Biophys. Acta 772 (1984) 357–373.
[12] F. Cornelius, Modulation of Na,K-ATPase and Na-ATPase activity by phospholipids and cholesterol. I. Steady-state kinetics, Biochemistry 40 (2001) 8842–8851.
[13] J.H. Ipsen, O.G. Mouritsen, G. Karlström, H. Wennerström, M.J. Zuckermann, Phase equilibria in the lechtin-cholesterol system, Biochim. Biophys. Acta 905 (1987) 162–172.
[14] J.M. East, D. Melville, A.G. Lee, Exchange rate and numbers of annular lipids for the calcium and magnesium ion dependent adenosinetriphosphatase, Biochemistry 24 (1985) 2615–2623.
[15] M. Esmann, D. Marsh, Lipid–protein interactions with the Na,K-ATPase, Chem. Phys. Lipids 141 (2006) 94–104.
[16] J.R. Brotherus, O.H. Griffith, M.O. Brotherus, P.C. Jost, J.R. Silvius, L.E. Hokin, Lipid–protein multiple binding equilibria in membranes, Biochemistry 20 (1981) 5261–5267.
[17] M. Esmann, A. Watt, D. Marsh, Spin-label studies of lipid–protein interactions in ($Na^+ + K^+$)-ATPase membranes from *Squalus acanthias*, Biochemistry 24 (1985) 1386–1393.

[18] J.R. Silvius, D.A. McMillen, N.D. Saley, P.C. Jost, O.H. Griffith, Competition between cholesterol and phosphatidylcholine for the hydrophobic surface of sarcoplasmic reticulum Ca^{2+}-ATPase, Biochemistry 23 (1984) 538–547.

[19] M. Laursen, L. Yatime, P. Nissen, N.U. Fedosova, Crystal structure of the high-affinity Na+, K+-ATPase-ouabain complex with Mg2+ bound in the cation binding site, Proc. Natl. Acad. Sci. U. S. A. 110 (2013) 10958–10963.

[20] O.G. Mouritsen, M. Bloom, Mattress model of lipid–protein interactions in membranes, Biophys. J. 46 (1984) 141–153.

[21] Y. Sonntag, M. Musgaard, C. Olesen, B. Schiøtt, J.V. Møller, P. Nissen, L. Thøgersen, Mutual adaptation of a membrane protein and its lipid bilayer during conformational changes, Nat. Commun. 2 (2011) 304.

[22] S. Yoda, A. Yoda, Phosphorylated intermediates of Na, K-ATPase proteoliposomes controlled by bilayer cholesterol, J. Biol. Chem. 262 (1987) 103–109.

[23] F. Cornelius, N. Turner, H.R. Christensen, Modulation of NaK-ATPase by phospholipids and cholesterol. II. Steady-state and presteady-state kinetics, Biochemistry 42 (2003) 8441–8549.

[24] F. Cornelius, Incorporation of C12E8-solubilized Na+, K+-ATPase into liposomes: determination of sidedness and orientation, Methods Enzymol. 156 (1988) 156–167.

[25] A.P. Starling, J.M. East, A.G. Lee, Effects of phosphatidylcholine fatty acyl chain length on calcium binding and other functions of the (Ca^{2+}-Mg^{2+})-ATPase, Biochemistry 32 (1993) 1593–1600.

[26] L. Miao, M. Nielsen, J. Thewalt, J.H. Ipsen, M. Bloom, M.J. Zuckermann, O.G. Mouritsen, From lanosterol to cholesterol: structural evolution and differential effects on lipid bilayers, Biophys. J. 82 (2002) 1429–1444.

[27] F. Cornelius, Cholesterol modulation of molecular activity of reconstituted shark Na+, K+-ATPase, Biochim. Biophys. Acta 1235 (1995) 205–212.

[28] G.B. Warren, M.D. Houslay, J.C. Metcalfe, N.J.M. Birdsall, Cholesterol is excluded from the phospholipid annulus surrounding an active calcium transport protein, Nature 255 (1975) 684–687.

[29] A. Johannson, G.A. Smith, J.C. Metcalfe, The effect of bilayer thickness on the activity of (Na^++K^+)-ATPase, Biochem. J. 196 (1981) 505–511.

[30] A.P. Starling, J.M. East, A.G. Lee, Effects of phospholipid fatty acyl chain length on phosphorylation and dephosphorylation of the Ca^{2+}-ATPase, Biochem. J. 310 (1995) 875–879.

[31] K.-H. Cheng, J.R. Lepock, S.W. Hui, P.L. Yeagle, The role of cholesterol in the activity of reconstituted Ca-ATPase vesicles containing unsaturated phosphatidylethanolamine, J. Biol. Chem. 261 (1986) 5081–5087.

[32] M.F. Brown, Influence of non-lamellar-forming lipids on rhodopsin, Curr. Top. Membr. 44 (1997) 285–356.

[33] R.S. Cantor, The influence of membrane lateral pressures on simple geometric models of protein conformational equilibria, Chem. Phys. Lipids 101 (1999) 45–56.

[34] F. Cornelius, Cholesterol-dependent interaction of polyunsaturated phospholipids with Na, K-ATPase, Biochemistry 47 (2008) 1652–1658.

[35] B.J. Litman, D.C. Mitchell, A role for phospholipid polyunsaturation in modulating protein functions, Lipids 31 (1996) S193–S197.

[36] D.C. Mitchell, B.J. Litman, Effect of cholesterol on molecular order and dynamics in highly polyunsaturated phospholipid bilayers, Biophys. J. 75 (1998) 896–908.

[37] J. Gullingsrud, K. Schulten, Lipid bilayer pressure profiles and mechanosensitive channel gating, Biophys. J. 86 (2004) 3496–3509.

[38] N.D. Drachmann, C. Olesen, Møller, Z. Guo, P. Nissen, M. Bublitz, Comparing crystal structures of Ca^{2+}-ATPase in the presence of different lipids, FEBS J. 281 (2014) 4249–4262.

[39] T. Murata, I. Yamota, Y. Kakinuma, A.G. Leslie, J.E. Walker, Structure of the rotor of the V-type Na^+-ATPase from *Enterococcus hirae*, Science 308 (2005) 654–659.

[40] K.E. McAuley, P.K. Fyfe, J.P. Ridge, N.W. Isaacs, R.J. Cogdell, M.R. Jones, Structural details of an interaction between cardiolipin and an integral membrane protein, Proc. Natl. Acad. Sci. U. S. A. 96 (2000) 14706–14711.

[41] L.-O. Essen, R. Siegert, W.D. Lehmann, D. Oesterhelt, Lipid patches in membrane protein oligomers: crystal structure of the bacteriorhodopsin-lipid complex, Proc. Natl. Acad. Sci. U. S. A. 95 (1998) 11673–11678.

[42] T. Tsukihara, H.B. Aoyama, E. Yamashita, T.B. Tomizaki, H. Yamaguchi, K. Shinzawa-Itoh, R. Nakashima, R. Yaono, S. Yoshikawa, The whole structure of the 13-subunit oxidized cytochrome *c* oxidase at 2.8 angstrom, Science 272 (1996) 1136–1144.

[43] P.M. Marius, M. Zagnoni, M.E. Sandison, J.M. East, H. Morgan, A.G. Lee, Binding of anionic lipids to at least three nonannular sites on the potassium channel KcsA is required for channel opening, Biophys. J. 94 (2008) 1689–1698.

[44] P.K. Fyfe, K.E. McAuley, A.W. Roszak, N.W. Isaacs, R.J. Cogdell, M.R. Jones, Probing the interface between membrane proteins and membrane lipids by X-ray crystallography, Trends Biochem. Sci. 26 (2001) 106–112.

[45] F. Cornelius, Y.A. Mahmmoud, Modulation of FXYD interaction with Na, K-ATPase by anionic phospholipids and protein kinase phosphorylation, Biochemistry 46 (2007) 2371–2379.

[46] C. Toyoshima, S. Yonekura, J. Tsueda, S. Iwasawa, Trinitrophenyl derivatives bind differently from parent adenine nucleotides to Ca^{2+}-ATPase in the absence of Ca^{2+}, Proc. Natl. Acad. Sci. U. S. A. 108 (2011) 1833–1838.

[47] K.P. Wheeler, R. Whittam, The involvement of phosphatidylserine in adenosine triphosphatase activity of the sodium pump, J. Physiol. 207 (1970) 303–328.

[48] Y. Hayashi, K. Mimura, H. Matsui, T. Takagi, High-performance gel chromatography of active solubilized Na+, K+-ATPase maintained by exogenous phosphatidylserine, Prog. Clin. Biol. Res. 268A (1988) 205–210.

[49] K. Mimura, H. Matsui, T. Takagi, Y. Hayashi, Change in oligomeric structure of solubilized Na^+/K^+-ATPase induced by octaethylene glycol dodecyl ether, phosphatidylserine and ATP, Biochim. Biophys. Acta 1145 (1993) 63–74.

[50] N. Shinji, Y. Tahara, E. Hagiwara, T. Kobayashi, K. Mimura, H. Takenaka, Y. Hayashi, ATPase activity and oligomerization of solubilized Na^+/K^+-ATPase maintained by synthetic phosphatidylserine, Ann. N. Y. Acad. Sci. 986 (2003) 235–237.

[51] S.J. Karlish, R. Goldshleger, W.D. Stein, A 19-kDa C-terminal tryptic fragment of the alpha chain of Na/K-ATPase is essential for occlusion and transport of cations, Proc. Natl. Acad. Sci. U. S. A. 87 (1990) 4566–4570.

[52] M. Esmann, A. Arora, A.B. Maunsbach, D. Marsh, Structural characterization of Na, K-ATPase from shark rectal glands by extensive trypsinization, Biochemistry 45 (2006) 954–963.

[53] P.L. Yeagle, J. Young, D. Rice, Effects of cholesterol on (Na+, K+)-ATPase ATP hydrolyzing activity in bovine kidney, Biochemistry 27 (1988) 6449–6452.

[54] D. Strugatsky, R. Goldshleger, E. Bibi, S.J. Karlish, Expression of Na, K-ATPase in P. pastoris: Fe2+-catalyzed cleavage of the recombinant enzyme, Ann. N. Y. Acad. Sci. 986 (2003) 247–248.

[55] E. Cohen, R. Goldshleger, A. Shainskaya, D.M. Tal, C. Ebel, M. le Maire, S.J.D. Karlish, Purification of Na+, K+-ATPase expressed in Pichia pastoris reveals an essential role of phospholipid–protein interactions, J. Biol. Chem. 280 (2005) 16610–16618.

[56] H. Haviv, E. Cohen, Y. Lifshitz, D.M. Tal, R. Goldshleger, S.J.D. Karlish, Stabilization of Na+, K+-ATPase purified from Pichia pastoris membranes by specific interactions with lipids, Biochemistry 46 (2007) 12855–12867.

[57] Y. Lifshitz, E. Petrovich, H. Haviv, R. Goldshleger, D.M. Tal, H. Garty, S.J.D. Karlish, Purification of the human alpha2 Isoform of Na, K-ATPase expressed in Pichia pastoris. Stabilization by lipids and FXYD1, Biochemistry 46 (2007) 14937–14950.

[58] A. Katz, Y. Lifshitz, E. Bab-Dinitz, E. Kapri-Pardes, R. Goldshleger, D.M. Tal, S.J.D. Karlish, Selectivity of digitalis glycosides for isoforms of human Na,K-ATPase, J. Biol. Chem. 285 (2010) 19582–19592.

[59] E. Kapri-Pardes, A. Katz, H. Haviv, Y. Mahmmoud, M. Ilan, I. Khalfin-Penigel, S. Carmeli, O. Yarden, S.J.D. Karlish, Stabilization of the alpha2 isoform of Na, K-ATPase by mutations in a phospholipid binding pocket, J. Biol. Chem. 286 (2011) 42888–42899.

[60] N.K. Mishra, Y. Peleg, E. Cirri, T. Belogus, Y. Lifshitz, D.R. Voelker, H.J. Apell, H. Garty, S.J.D. Karlish, FXYD proteins stabilize Na, K-ATPase: amplification of specific phosphatidylserine-protein interactions, J. Biol. Chem. 286 (2011) 9699–9712.

[61] J. Fantini, F.J. Barrantes, How cholesterol interacts with membrane proteins: an exploration of cholesterol-binding sites including CRAC, CARC, and tilted domains, Front. Physiol. 4 (2013) 31.

[62] N.P. Barrera, M. Zhou, C.V. Robinson, The role of lipids in defining membrane protein interactions: insights from mass spectrometry, Trends Cell Biol. 23 (2013) 1–8.

[63] A. Laganowsky, E. Reading, T.M. Allison, M.B. Ulmschneider, M.T. Degiacomi, A.J. Baldwin, C.V. Robinson, Membrane proteins bind lipids selectively to modulate their structure and function, Nature 510 (2014) 172–175.

[64] H. Garty, S.J. Karlish, Role of FXYD proteins in ion transport, Annu. Rev. Physiol. 68 (2006) 431–459.

[65] K. Geering, FXYD proteins: new regulators of Na-K-ATPase, Am. J. Physiol. Renal Physiol. 290 (2006) F241–F250.

[66] J.J. de Pont, A. van Prooijen-van Eeden, S.L. Bonting, Role of negatively charged phospholipids in highly purified (Na^++K^+)-ATPase from rabbit kidney outer medulla studies on (Na^++K^+)-activated ATPase, XXXIX, Biochim. Biophys. Acta 508 (1978) 464–477.

[67] D.H. Jones, T.Y. Li, E. Arystarkhova, K.J. Barr, R.K. Wetzel, J. Peng, K. Markham, K.J. Sweadner, G.H. Fong, G.M. Kidder, Na, K-ATPase from mice lacking the gamma subunit (FXYD2) exhibits altered Na+ affinity and decreased thermal stability, J. Biol. Chem. 280 (2005) 19003–19011.

[68] C. Donnet, E. Arystarkhova, K.J. Sweadner, Thermal denaturation of the Na, K-ATPase provides evidence for alpha-alpha oligomeric interaction and gamma subunit association with the C-terminal domain, J. Biol. Chem. 276 (2001) 7357–7365.

[69] R. Goldshleger, D.M. Tal, S.J. Karlish, Topology of the alpha-subunit of Na,K-ATPase based on proteolysis. Lability of the topological organization, Biochemistry 34 (1995) 8668–8679.

[70] P.L. Jorgensen, J.P. Andersen, Thermoinactivation and aggregation of alpha beta units in soluble and membrane-bound (Na, K)-ATPase, Biochemistry 25 (1986) 2889–2897.

[71] P.L. Jorgensen, Purification of Na+, K+-ATPase: enzyme sources, preparative problems, and preparation from mammalian kidney, Methods Enzymol. 156 (1988) 29–43.

[72] I. Mangialavori, M.R. Montes, R.C. Rossi, N.U. Fedosova, J.P.F.C. Rossi, Dynamic lipid–protein stoichiometry on E1 and E2 conformations of the Na+, K+-ATPase, FEBS Lett. 585 (2011) 1153–1157.

[73] J.R. Nealon, S.J. Blanksby, T.W. Mitchell, P.L. Else, Systematic differences in membrane acyl composition associated with varying body mass in mammals occur in all phospholipid classes: an analysis of kidney and brain, J. Exp. Biol. 211 (2008) 3195–3204.

[74] M. Liang, J. Tian, L. Liu, S. Pierre, J. Liu, J. Shapiro, Z.J. Xie, Identification of a pool of non-pumping Na/K-ATPase, J. Biol. Chem. 282 (2007) 10585–10593.